

Late Cenozoic tectonic evolution of the northwestern Tien Shan: New age estimates for the initiation of mountain building

M.E. Bullen*

D.W. Burbank†

Department of Geosciences, Pennsylvania State University, Deike Building, University Park, Pennsylvania 16801, USA

J.I. Garver

Geology Department, Union College, Olin Building, Schenectady, New York 12308, USA

K.Ye. Abdrakhmatov

Kyrgyz Institute of Seismology, Kyrgyz Academy of Sciences, Asanabai 52/1, Bishkek 720060, Kyrgyzstan

ABSTRACT

The Tien Shan are the quintessential intracontinental range, situated more than 1000 km north of the suture between India and Asia. Their initiation and growth in the Cenozoic, however, remain poorly understood. In this study we present stratigraphic, detrital fission-track, and magnetostratigraphic results that provide a basis for reconstructing the Cenozoic tectonic evolution of the Kyrgyz Range and adjacent Chu basin in the northwestern Tien Shan. Detrital fission-track thermochronology indicates that the northwestern Tien Shan was tectonically quiescent for much of the Cenozoic. Prior to uplift and exhumation in the late Miocene, the Kyrgyz Range was buried by sediments shed from highlands to the south and/or east. Paired bedrock fission-track and [U-Th]/He ages from a sampling transect of 2.4 km relief demonstrate that rapid exhumation commenced at ca. 11 Ma. Initial thrusting in the hinterland was followed by evaporite accumulation (~0.4 km/m.y.), which coincided with erosion of the pre-11 Ma strata that mantled the Kyrgyz Range. Between 10 and 3 Ma, bedrock-exhumation rates decreased to <0.3 km/m.y., while sedimentation rates decelerated initially to ~0.25 km/m.y. before accelerating to ~0.4 km/m.y. at 4–5 Ma. Detrital fission-track results indicate that by 4.5 Ma,

the top of an exhumed apatite partial annealing zone (PAZ) was exposed in the Kyrgyz Range, corresponding with ~2 km of total exhumation. Continued exhumation of the Kyrgyz Range resulted in exposure of fully reset rocks from below the exhumed PAZ (~4–5 km depth) by ca. 1.5 Ma. Fission-track ages from two modern stream samples collected ~75 km apart along the range front indicate that exhumation in the Kyrgyz Range commenced in the west and then propagated to the east.

Keywords: Central Asia, erosion, fission-track, magnetostratigraphy, Tien Shan.

INTRODUCTION

There are few better localities at which to study the style and rate of intracontinental mountain building than the Tien Shan of Central Asia (Fig. 1). If for no other reason, the Tien Shan are noteworthy because their development in the Miocene is a direct result of the collision of India with Asia: an event that started some 55 m.y. ago and 1000–2000 km to the south. Despite the remote position of the Tien Shan with respect to the Himalaya, GPS (Global Positioning System) data indicate that ~40% of the present-day shortening between India and Asia can be accounted for in the western Tien Shan (Abdrakhmatov et al., 1996). Determining the beginning of mountain building and the fluctuation of strain rates within the Tien Shan is key to addressing unresolved issues regarding the evolution of the Himalaya orogen. Establishing an initiation age for the western Tien Shan provides a framework for better understanding the rate at

which strain was transmitted from the Indo-Asian collisional front, places bounds on the timing and preeminence of movement along major strike-slip systems (Altyn Tagh and Kunlun faults), and tests the causal relationship between uplift of the Tibetan Plateau and development of the Tien Shan (Burtman et al., 1996; Abdrakhmatov et al., 1996).

Although earlier studies were hampered by a paucity of temporal and structural information (Windley et al., 1990), estimates on the initiation and style of shortening in the Tien Shan proliferated in the 1990s (Allen et al., 1993; Avouac et al., 1993; Hendrix et al., 1994; Abdrakhmatov et al., 1996; Metivier and Gaudemer, 1997; Sobel and Dumitru, 1997; Yin et al., 1998). Many of these studies, however, are either reconnaissance in nature or focus primarily on the eastern or southern Tien Shan. The northwestern Tien Shan is noted for its east-trending ranges with elevations in excess of 4 km and intervening intermontane basins containing well-exposed Cenozoic strata up to 6 km thick (Fig. 1). The study of such hinterland-foreland couplets has long been acknowledged as the key to reconstructing the timing of thrust initiation (e.g., Burbank and Reynolds, 1988; Jordan et al., 1988), progressive bedrock unroofing (e.g., DeCelles et al., 1991), and basin geometry and subsidence (e.g., Flemings and Jordan, 1989). The northwestern Tien Shan is, therefore, an ideal natural laboratory for answering fundamental questions concerning the tectonic development of the Tien Shan.

The Kyrgyz Range and adjacent Chu basin mark the northernmost extent of the western Tien Shan (Fig. 1). Although several studies

*Present address: ExxonMobil Exploration Company, GP3, Benmar Street, Houston, Texas 77060, USA; e-mail: michael.e.bullen@exxon.sprint.com.

†Present address: Department of Geological Sciences, Building 526, University of California, Santa Barbara, California 93106-9630, USA.

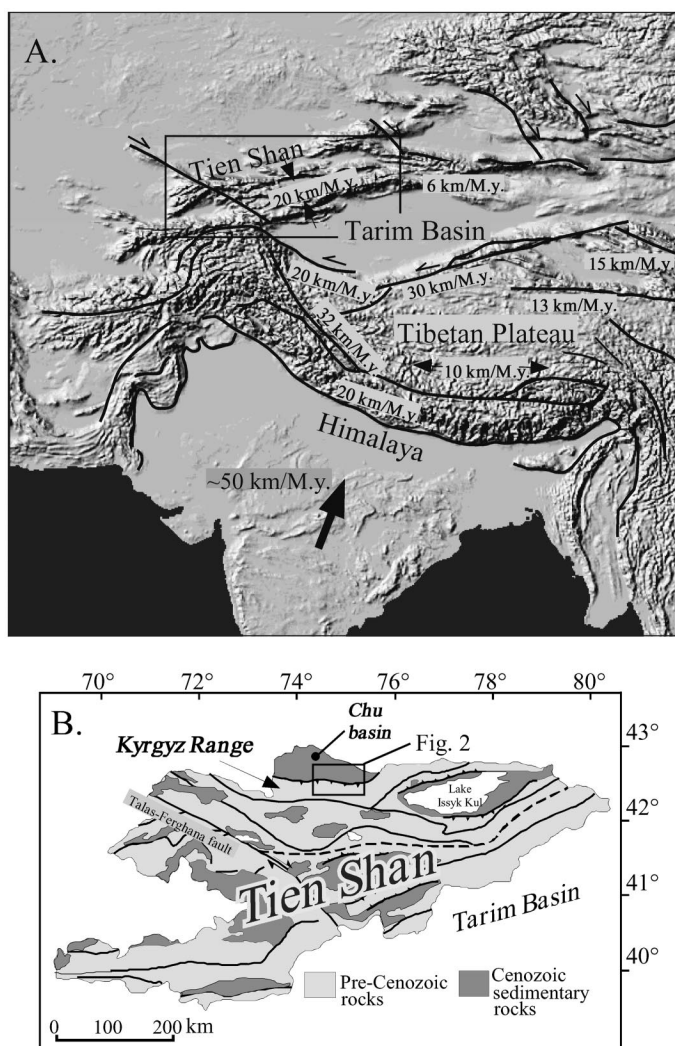


Figure 1. (A) Regional tectonic map of Central Asia showing Holocene partitioning of strain associated with convergence of India (after Avouac et al., 1993). (B) Simplified geology of Kyrgyzstan. Location shown by box in A.

have catalogued the regional stratigraphy and thrust kinematics of this area (Ibragimov and Turdukulov, 1965; Tarasov, 1971; Chediya et al., 1973; Fortuna, 1973; Trofimov et al., 1976), few have actually documented the relationships between uplift, exhumation, and basin deposition. In this study, we compare rates of exhumation in the Kyrgyz Range (Bullen, 1999) with the accumulation history and facies architecture in the adjacent Chu foreland basin to better understand the timing and style of mass transfer during the Miocene and Pliocene. We present the first thermochronologic data for the northwestern Tien Shan, employing magnetostratigraphy and detrital fission-track dating (Figs. 1, 2, and 3). The synthesis of these results suggests that the northwestern Tien Shan underwent complex

and variable growth from 11 Ma to the present.

TECTONIC SETTING

The Tien Shan record two Paleozoic collisional events—one along the southern margin of the range (Late Devonian–early Carboniferous [Mississippian]) and a second along the northern margin (late Carboniferous [Pennsylvanian]–Early Permian) (Burtman, 1975; Windley et al., 1990; Allen et al., 1992; Carroll et al., 1995). The first event involved the collision of the Tarim block with the central Tien Shan, a continental fragment, which was at this time still separated from the Asian landmass (Allen et al., 1992; Carroll et al., 1995). Approximately 70 m.y. later, the northern Tien

Shan island arc was accreted to the northern margin of the combined Tarim–central Tien Shan continental block, effectively closing the paleo-ocean basin. By the Early Permian, Central Asia was fully amalgamated (Burtman, 1975; Windley et al., 1990; Avouac et al., 1993), after which time a less-active tectonic regime prevailed until the collision of India in the early Tertiary (ca. 50–55 Ma).

An exception to this period of relative quiescence is faulting during the Triassic and Jurassic (Burtman, 1980; Hendrix et al., 1992; Burtman et al., 1996). Thick Triassic and Lower to Middle Jurassic strata crop out in the Turpan, Junggar, and northern Tarim Basins, and their deposition has been linked to episodic fault movement (Hendrix et al., 1992). Although isolated vestiges of Jurassic deposits remain along the flanks of a few intermontane basins in the west, they are not comparable in thickness or extent with those found in the eastern Tien Shan. Paleogeographic reconstructions for the Jurassic depict clastic input from the northern Tien Shan into intermontane basins in the central and southern parts of the Tien Shan (Atlas Kyrgyzskoi CCP I, 1987). We infer from these reconstructions that the northern Tien Shan was exhumed a modest amount in the Jurassic.

The Tien Shan remained tectonically inactive for much of the Late Cretaceous and Cenozoic, including some 30–40 m.y. after the collision of India in the early Eocene. This long period of stability and tectonic inactivity resulted in the beveling of topography and a decrease of local relief (Norin, 1941; Burtman, 1975; Bally et al., 1986). In the western Tien Shan, this period of quiescence is characterized by paleosols and carbonate-cemented breccias known as the Kokturpak Formation (Chediya et al., 1973). This unit was deposited as discontinuous pockets of strata directly on top of the beveled Paleozoic substrate. Basalt dikes that cut the Kokturpak Formation have been dated by the K-Ar method at 55 Ma (Krylov, 1960), which when combined with existing faunal evidence, suggests that the lowermost Kokturpak is Cretaceous(?) to Paleogene in age (Chediya et al., 1973).

In addition to the regionally extensive angular unconformity at the base of the Kokturpak Formation, a late Oligocene–early Miocene unconformity is documented within the Cenozoic strata. In the northwestern Tien Shan, coarser-grained clastic strata lie unconformably above multicolored mudstone and limestone, a relationship interpreted to represent the initiation of regional deformation (Chediya et al., 1973). An unconformity similar in character, but with a poorly defined age,

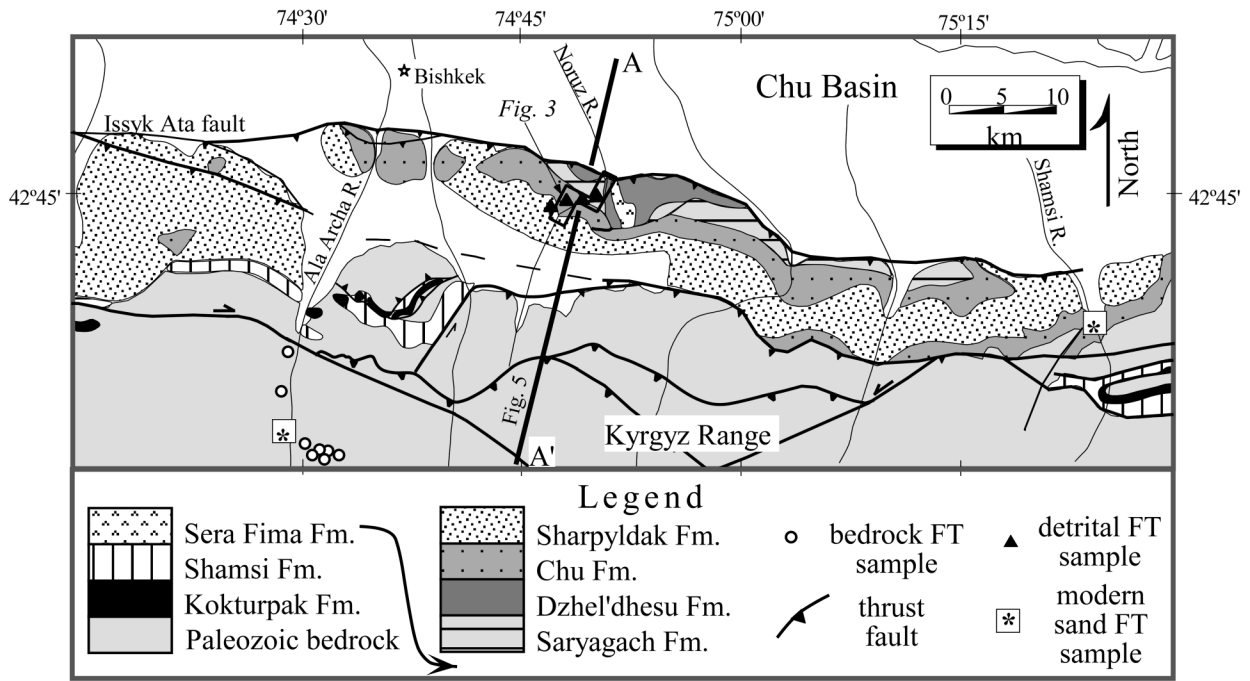


Figure 2. Geologic map of the Chu basin and adjacent Kyrgyz Range (modified after Trofimov et al., 1976, Mikolaichuk, 2000). Section A-A' is shown in Figure 5.

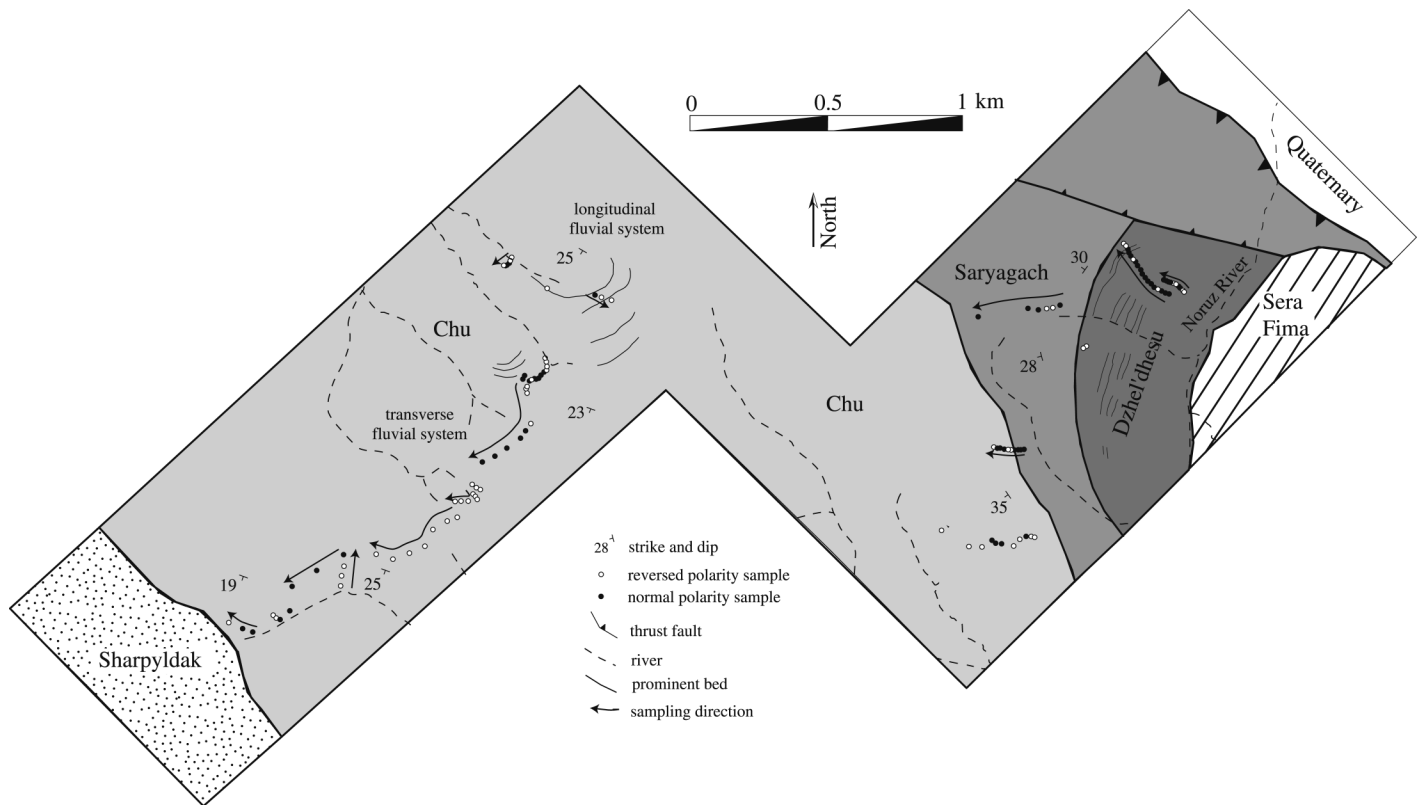


Figure 3. Detailed site location map for magnetostratigraphic section along the west side of the Noruz River. For location, see Figure 2.

is also documented ~1000 km east near Urumqi (Hao and Zeng, 1984; Windley et al., 1990; Allen et al., 1993; Avouac et al., 1993).

Some of the world's largest earthquakes ($M > 8$) in the twentieth century occurred in the Tien Shan (Molnar and Deng, 1984; Ghose et al., 1997). Aftershocks suggest that active faults extend to mid-crustal depths (~18 km) along fault planes with uniform dip (~45°–50°) (Ghose et al., 1997). Although many of these active structures are located at the margins of east-trending intermontane basins, a considerable component of strain is also being accommodated by younger fault systems that have recently propagated into the basin centers. This deformation is manifested in high modern shortening rates (Abdrakhmatov et al., 1996), folded fluvial terraces (Avouac et al., 1993), and exposed fault scarps (Avouac et al., 1993; Ghose et al., 1997; Brown et al., 1998; Thompson et al., 1999).

INITIATION OF MOUNTAIN BUILDING

Many workers have presented estimates for the initiation and growth rate of the Tien Shan (Windley et al., 1990; Allen et al., 1993; Avouac et al., 1993; Hendrix et al., 1994; Yin et al., 1998). Herein we summarize the most important age estimates and regional control.

Conglomerate deposition above a late Oligocene–early Miocene unconformity has been used to loosely bracket the onset of synorogenic deposition in the Tien Shan (Chediya et al., 1973; Windley et al., 1990; Allen et al., 1993). However, both the age of the unconformity and that of the detritus above it remain poorly resolved. Metivier and Gaudemer (1997) improved upon this late Oligocene–early Miocene initiation estimate by reconstructing the temporal and spatial depositional history of the Tarim and Junggar Basins. This study delimited two main pulses in sediment accumulation at ca. 17 and 5–6 Ma. Metivier and Gaudemer (1997) proposed that the 17 Ma event recorded local deposition in the northern Tarim Basin associated with the initiation of thrusting along the southern Tien Shan. However, this estimate suffers from a paucity of subsurface and chronologic control.

Thermochronologic and stratigraphic evidence from the southern and eastern Tien Shan indicate an early Miocene initiation of deformation (Hendrix et al., 1994; Sobel and Dumitru, 1997; Yin et al., 1998). Late Oligocene–middle Miocene (25–13 Ma) fission-track ages from the southern Tien Shan and northeastern Pamir Mountains document the progressive unroofing of Tien Shan thrust sys-

tems (Sobel and Dumitru, 1997). Facies changes suggest a minimum initiation age of 21–24 Ma of the Kuche thrust system in the southern Tien Shan (Yin et al., 1998). In the eastern Tien Shan, Hendrix et al. (1994) dated three partially annealed detrital samples with a component of 24 Ma apatite grains. The similarity in timing of these estimates with slowed left-slip movement along the Red River fault, increased exhumation of the Himalaya, and movement along the Main Central thrust and South Tibetan detachment system has led workers to conclude that growth of the Tien Shan commenced after a change from extrusion-dominated to crustal-thickening-dominated strain accommodation in the Himalaya and Pamir Mountains (Hendrix et al., 1994; Sobel and Dumitru, 1997).

Early Miocene estimates for the initiation of deformation in the Tien Shan stand in contrast to interpretations based on geodetic rates. Estimates of total shortening near Urumqi (~200 ± 50 km) and extrapolated geodetically determined modern shortening rates (20 km/m.y.) imply that the Tien Shan was constructed in the past 10 m.y. (Avouac et al., 1993; Abdrakhmatov et al., 1996). Similarly, Cenozoic slip on the Talas-Ferghana fault is estimated at <100 km, and fault slip has accumulated at rates of ~10 km/m.y., suggesting that deformation commenced more recently than ca. 10 Ma (Burtman et al., 1996). These studies assert that the attainment of maximum elevation of the Tibetan Plateau may have changed the regional stress field at ca. 8 Ma (Molnar et al., 1993), which in turn led to the construction of the Tien Shan (Abdrakhmatov et al., 1996; Burtman et al., 1996).

STRATIGRAPHY OF THE CHU BASIN

This study focuses on the hinterland-foreland couplet of the Kyrgyz Range and adjacent Chu basin (Fig. 2). Much of the Kyrgyz Range is cored by Ordovician granite and fine-grained Devonian sedimentary rocks and is cut by numerous short, irregular imbricate thrust faults that are laterally truncated by throughgoing strike-slip faults (Fig. 2) (Atlas Kyrgyzskoi CCP I, 1987). The Paleozoic bedrock is thrust northward over ~4 km of Cenozoic molasse at the margin of the Chu basin, a small flexural basin some 50 km wide and 150 km long (Fig. 4) (Trofimov et al., 1976; IVTAN [Institute for High Temperatures of the Russian Academy of Sciences], 1983). The deformation front stepped northward into the Chu basin, exposing a thick succession of Neogene strata along the Issyk-Ata

fault, located ~10 km north of the basin-margin structures (Fig. 2).

Noruz Structural and Stratigraphic Section

The thickest and most complete Tertiary stratigraphic section exposed in the Chu basin is along the west side of the Noruz River (Fig. 2). Unlike the simple homoclinally south-dipping strata along strike, local salt-clay diapirism in the Noruz region has created a tip-line anticline, exposing >3 km of Cenozoic strata. Active displacement along the Issyk Ata fault marks the youngest phase of deformation within the region, tilting the Noruz section into a continuous dip panel 25°–30°. If we assume that the fault plane is parallel to the panel, then translation of this ~3–4-km-thick sediment package up an ~30° ramp is equivalent to ~6 km of horizontal shortening (Fig. 5). Considering that shortening rates for the Issyk Ata fault are 0.2–0.35 km/m.y., as derived from a fault trenching study (Chediya et al., 1998), the ~6 km of shortening commenced within the past ~2–3 m.y.

A generalized stratigraphic column comprising seven Tertiary formations totals ~6 km in thickness (from bottom to top): (1) Kokturpak, (2) Kokmeren, (3) Sera Fima, (4) Dzhel'dysu, (5) Saryagach, (6) Chu, and (7) Sharpyldak (Ibragimov and Turdukulov, 1965; Tarasov, 1971; Chediya et al., 1973) (Fig. 2). In this study, we sampled only the upper four formations, which constitute a 3.1-km-thick upward-coarsening section (Figs. 6 and DR1 [Data Repository Fig. 1]).¹ The basal three formations are not exposed in the Noruz region, but are described from drill-core records and exposures elsewhere in the Chu basin (Chediya et al., 1973).

In the region of the Noruz anticline, the Kokturpak Formation unconformably rests upon a 5-m-thick residual soil developed on Late Devonian volcanic rocks. The Kokturpak Formation, an ~0.6-km-thick variegated claystone with lenses of fine-grained sandstone and interlayers of nonmarine carbonate and anhydrite, is interpreted to represent the redistribution of the residual soil (Chediya et al., 1973). The thickness of the Kokturpak Formation in the Noruz region is atypical for the Chu basin, where deposits are generally <0.15 km thick.

The 1.3-km-thick Kokmeren Formation

¹GSA Data Repository item 2001134 is available on the Web at <http://www.geosociety.org/pubs/ft2001.htm>. Requests may also be sent to editing@geosociety.org.

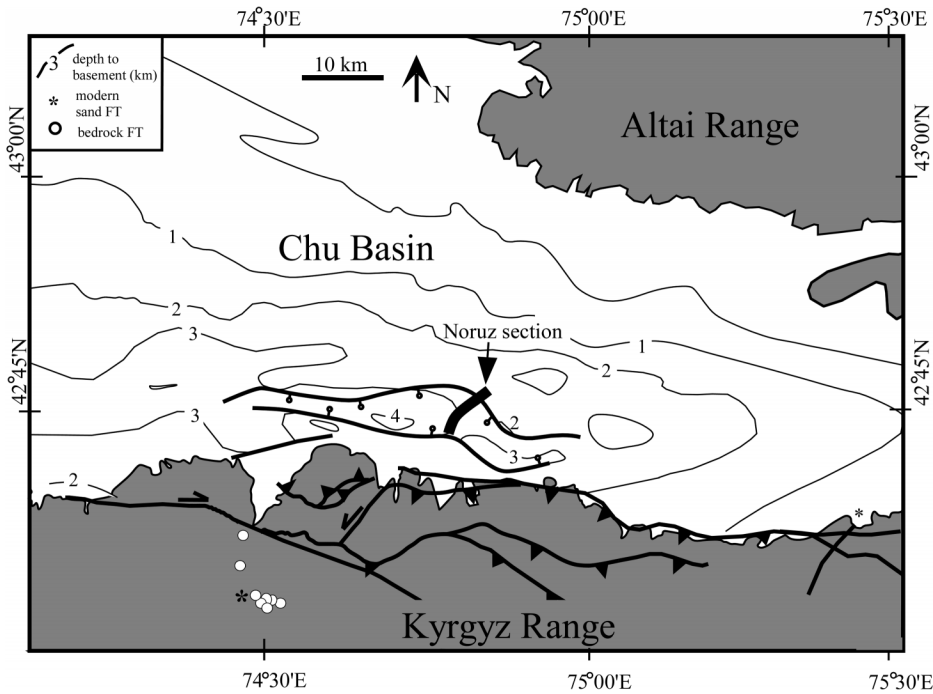


Figure 4. Structural map showing the top of Paleozoic basement in the Chu basin. Note the general asymmetry of the basin implying that basin formation resulted at least in part from tectonic loading by the Kyrgyz Range. White circles and asterisks indicate locations of bedrock fission-track (FT) and modern stream samples, respectively. Detrital samples were collected from the Noruz section. Structure modified after Trofimov et al. (1976) and depth to basement after IVTAN (Institute for High Temperatures of the Russian Academy of Sciences) (1983).

includes a lower unit (0.9 km) composed of “rhythmically interlayered, variegated siltstones and sandstones in approximately equal amounts.” Sandstone beds are described as quartzofeldspathic, fine to coarse grained, with “scattered interlayers, and patches of fine pebble and gravel-size fragments” (Chediya et al., 1973, p. 43). The upper unit (0.4 km) is slightly finer in character, comprising thinly bedded siltstone, sandstone, and fine-pebble conglomerate.

The Sera Fima Formation is composed of gray-green gypsiferous claystones with interbedded halite lenses. The thickness of the unit varies considerably (2.1 km to 0.5 km), owing to secondary remobilization that resulted from either salt or clay diapirism during displacement along the Issyk Ata fault and/or during sedimentation. In light of its limited lateral extent (~40 × 20 km), it is likely that this unit represents playa or restricted shallow-lake deposition.

Variegated mudstone and an increase in sand content distinguish the ~0.2-km-thick Dzhel’dysu Formation from the underlying Sera Fima Formation. Nonfossiliferous, gypsum-rich, oxidized mudstone beds at the base of the unit grade upward into 2–4-m-thick interlayers of homogeneous red and gray-green mudstone. Laterally extensive, massive, medium-grained sandstones, generally <1 m thick, occur near the top of the formation. We interpret this unit to have been deposited in an evaporitic playa-margin setting, as indicated by both the gypsum-rich mudstone and sporadic sheet-sand deposition. Bidirectional pa-

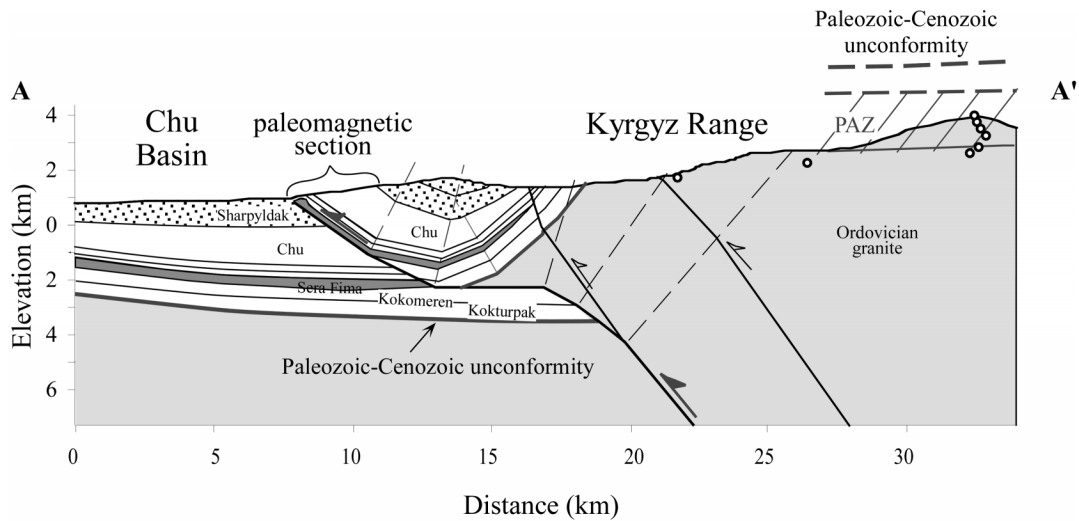


Figure 5. Balanced cross section of the Chu basin and Kyrgyz Range. Bedrock fission-track sample locations (from Bullen, 1999), shown as open circles, were projected along structural strike. The modern position of the relict apatite partial annealing zone (PAZ) is reconstructed on the basis of fission-track ages from the Kyrgyz Range (Bullen, 1999). Structure modified after Trofimov et al. (1976). Location of section A–A’ is shown in Figure 2.

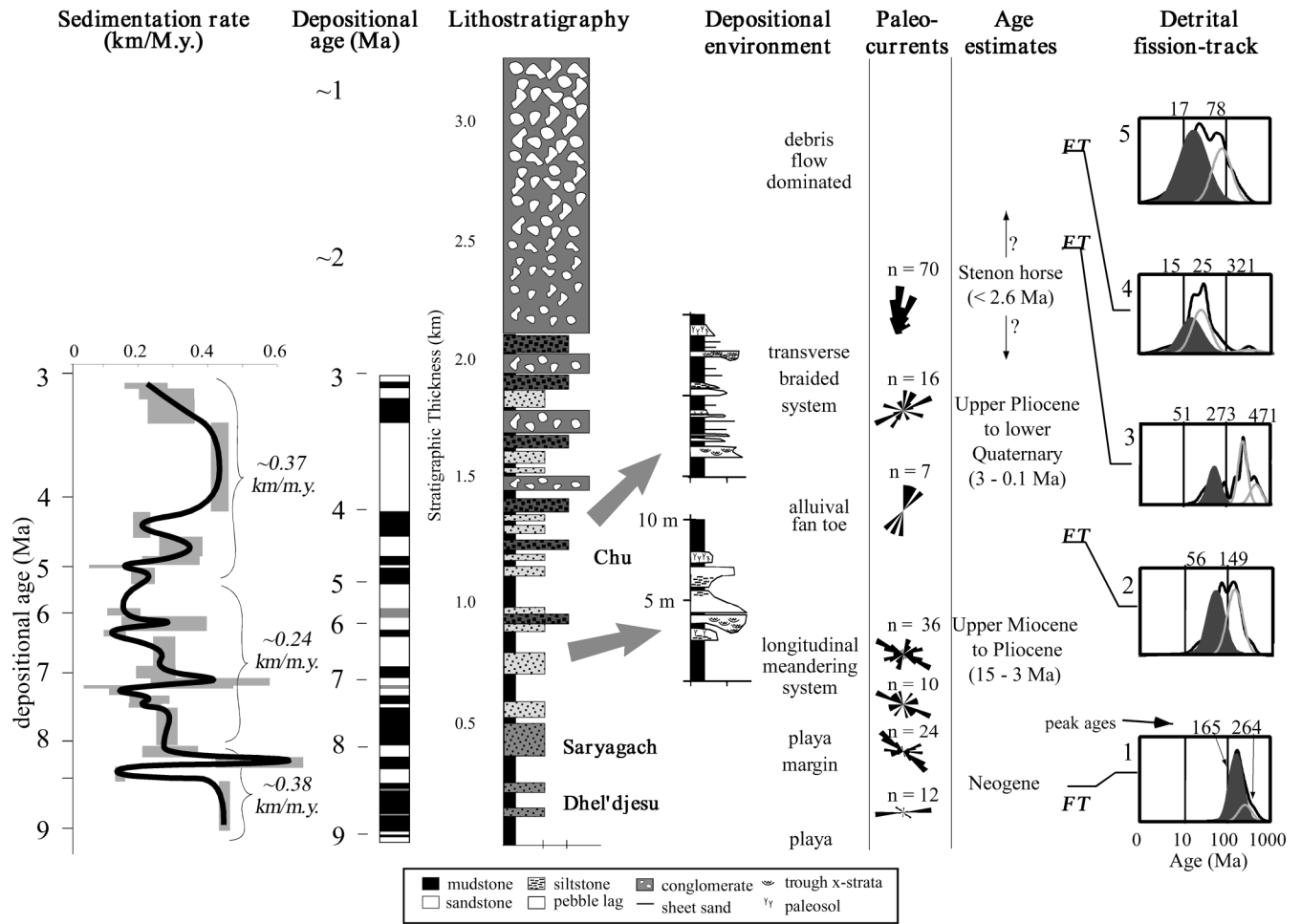


Figure 6. Compilation of all age and facies data collected from the Noruz catchment, Chu basin. Accumulation rates were calculated after correlation of the magnetostratigraphic section to the global polarity time scale (GPTS). Grain-age populations, or peaks, were statistically separated by using the routine of Brandon (1996). Youngest peaks, which are shaded gray, decrease in age upward through the section from 165 Ma to 15 Ma. Age estimates are from Chediya et al. (1973) and Trofimov et al. (1976). FT—fission track.

leocurrent data collected primarily from small channel scours indicate that the paleodrainage was oriented east-west.

The Saryagach Formation (0.2–0.5 km) is considerably coarser than the underlying units, exhibiting well-indurated, red, poorly sorted sandstone and pebbly conglomerate, with matrix-supported subangular clasts, and thin (5–10 m) multicolored (white, gray, and green) interbeds of calcareous siltstone. Individual sandstone and conglomerate units are laterally continuous and generally no thicker than 1–2 m; the clast sizes are <2 cm. Paleo-flow directions, gathered mostly from channel scours, cross-beds, and pebble imbrication, document flow toward the northwest (Fig. 6). We interpret that the Saryagach Formation was deposited at the interface of an alluvial fan and a playa-lake margin.

We divide the overlying Chu Formation

(1.5 km) into two subunits based on differences in both sedimentology and paleocurrents: (1) a lower mud-dominated unit (sandstone:shale = 1:4) with southeast or northwest paleo-flow directions and (2) an upper sand-dominated unit (sandstone:shale = 1.5:1) with a north-northwest paleo-flow direction. The lower unit is characterized by thick (<20 m) sequences of massive brown mudstone with thin (3–5 cm) interlayers of white, well-cemented calcareous concretions. Amalgamated channel deposits of 5–10 m thickness punctuate the homogeneous mudstone intervals. Channel-fill sequences typically coarsen upward, containing well-sorted, medium-grained sandstone capped by poorly sorted, coarse-grained, pebbly conglomerate and stringers of gravel lag. Paleocurrent data were collected from trough cross-beds and channel scours.

The upper unit comprises stacked, thin-bed-

ded (<2 m) massive sheet sandstone, red siltstone, and interlayers of white, well-cemented calcareous concretions. Although the percentage of sandstone is markedly increased in comparison to the lower Chu Formation, channel widths and the maximum grain size are approximately the same. Dense, gray, matrix-supported conglomerate beds are present in the middle of this unit, and, along with the sandstone beds, increase in abundance and thickness toward the top of the Chu Formation. The component clasts are well rounded, moderate to well sorted, up to 15 cm in diameter, and commonly imbricated. The Chu Formation is interpreted to encompass a change from longitudinal (east-southeast to west-northwest) braided-river deposition to transverse (south-southeast to north-northwest) alluvial-fan deposition (Fig. 6). Longitudinal drainage in the lower unit is charac-

terized by laterally variable lithofacies with contemporaneous floodplain, overbank, and channel deposition. Thick mudstone deposits encapsulate vertically disconnected channel units, which may reflect high rates of vertical accretion (Bridge and Leeder, 1979; Bentham et al., 1993). The upper Chu Formation records progradation of a north-directed alluvial fan over the longitudinal deposits of the lower Chu Formation.

The Chu Formation passes transitionally into the Sharpyldak Formation, a 1.3-km-thick coarsening-upward unit composed primarily of coarse-pebble conglomerate. The lower part of the unit has amalgamated beds of dense cliff-forming conglomerate more than 100 m thick. This gray conglomerate grades upward into poorly sorted, matrix-supported fanglomerates with granitic boulders as large as 1 m in diameter. Both the upper and lower members of the Sharpyldak Formation show evidence for north-directed paleocurrents interpreted to represent continued progradation of transverse alluvial and debris-flow fans into the Chu basin.

Tectonic Significance of the Foreland Fill

The Kokturpak Formation has previously been interpreted to record initial deformation in the Tien Shan (Chediya et al. 1973). We suggest that the multiple unconformities and extensive cementation is more consistent with deposition in a highly condensed section resulting from episodic deposition on a low-relief landscape that was steadily beveled by erosion. It appears unlikely that the nearby Kyrgyz Range was the source of these sediments. About 15 km west of the Noruz section, a 0.1–0.2 km thickness of the Kokturpak Formation mantles the outer flanks of the range (Fig. 2), suggesting that the range itself was covered by this clastic material.

Local deposition of >0.5 km of evaporite (Sera Fima Formation) indicates that the Noruz region contained a small, but long-lasting closed-lake basin. Although fine-grained deposits have been genetically linked with various tectonic conditions, we recognize three potential mechanisms for deposition of the Sera Fima Formation: (1) rapid basin subsidence due to flexural loading (Beck et al., 1988; Heller et al., 1988); (2) erosion of fine-grained source rocks, and (3) distal deposition in front of an approaching thrust front.

The 3.1 km of measured and sampled clastic strata in the Noruz section are characterized by (1) upward coarsening and (2) paleocurrent reorientation (Figs. 6 and DR1). Clastic deposition of the Saryagach and lower

Chu Formations infilled the evaporitic Noruz depression and hence represent a fundamental change in depositional environment, basin geometry, and surface gradients. Similarly, the clastic strata of the upper Chu and Sharpyldak Formation represent the widespread dispersal of coarse fan facies. Although these attributes appear to indicate increasingly proximal tectonism, it is difficult to assess a sole cause, as fan progradation commonly accompanies thrust development (Burbank and Reynolds, 1988), climate change (Jordan et al., 1988), or isostatic rebound (Heller et al., 1988).

MAGNETOSTRATIGRAPHY

Analytical Procedure

Some 444 paleomagnetic samples were collected from 135 sample sites within a 1.9-km-thick stratigraphic section along the west bank of the Noruz River (Fig. 3). Three or more oriented red or brown mudstone or siltstone samples were collected from each site by using an impact corer. The average vertical spacing between sites was ~15 m. Samples were not collected in the conglomeratic Sharpyldak Formation owing to the paucity of fine-grained sedimentary rock. Characteristic remanence directions (ChRM) were revealed by step-wise thermal (TD) and alternating-field (AF) demagnetization. Approximately 30 randomly selected samples were chosen for a pilot study in which 12 AF (0–100 Oe) and 6 TD (100, 300, 450, 550, 650, 690 °C) steps were run. Most of these samples had a low-coercivity component and a high-coercivity component, which were removed by demagnetization between 100 Oe–100 °C and 300 Oe–600 °C, respectively (Fig. 7). However, most samples had stable remanence directions well above 300 °C, retaining as much as 60% of their initial remanence above 550 °C. On the basis of these high unblocking temperatures, we infer that the common mineral carrier is hematite. From the representative demagnetization paths, we used four AF steps (0, 25, 50, 100 Oe) and up to 6 TD steps on the remaining samples. The ChRM was defined by using a least-squares fitting method (Kirschvink, 1980).

On the basis of the k -statistic of dispersion of sample directions, sites were defined as either class I ($k > 10$), class II ($k < 10$), or class III (indeterminate polarity or $n = 1$) (Fisher, 1953). For class II sites, the polarity was unambiguous, but commonly only two of three individual samples displayed coherent directions. Class III sites were not used in our polarity determinations. Out of the 135 sample

sites, 56% were class I, 29% were class II, and 15% were class III. More than 50% of the class III sites were in the lower third of the section, where many samples were retrieved in friable material. We performed reversal and fold tests using only class I sites whose α_{95} error did not cross the 0° VGP (virtual geomagnetic pole) latitude. The data pass the C reversal test of McFadden and McElhinny (1990), with a critical angle (γ_c) of 11.5°, indicating that a secondary overprint was successfully removed (Fig. 8). Although clustering improved after unfolding (in situ $k = 6.4$; bedding-corrected $k = 8.5$), the data did not pass the fold test at the 95% confidence interval (Fig. 8). Because the strike and dip remain uniform throughout the sampled section (Fig. 3), we would not expect the data to pass a fold test. Therefore, given the large number of magnetic reversals and passage of the reversal test, we are confident that we have separated the characteristic remanence directions.

For each class I and II site, we calculated the paleolatitude of the VGP in order to define normal or reversed magnetozones. On the basis of these calculations, we recognize 32 magnetozones in the Noruz stratigraphic section (Fig. 9). Most of these magnetozones are defined by two or more sites. There are, however, five single-site reversals, of which three are defined by a class I site with a relatively high VGP latitude. The actual presence or absence of the remaining two single-site reversals would not affect our correlation to the geomagnetic polarity time scale (GPTS) (Cande and Kent, 1995).

Correlation to the Geomagnetic Polarity Time Scale

Without precise independent age estimates from isotopic or biostratigraphic data, correlation to the GPTS is challenging. In the Noruz section, a horse fossil was found within the gray conglomerate of the lower Sharpyldak Formation (Trofimov et al., 1976), <0.5 km above the top of our section. This fossil was identified as a primitive species of the horse *Equus* (Ray Bernor, 1999, personal commun.), which underwent rapid dispersal between North America and Asia beginning at ca. 2.6 Ma (Lindsay et al., 1980). Therefore, the horse fossil provides a maximum limiting age of 2.6 Ma for the lower Sharpyldak Formation. In the same conglomeratic formation, local researchers identified freshwater ostracods of late Pliocene age (Trofimov et al., 1976), thereby refining the age of the Sharpyldak Formation to ca. 3.5–1.5 Ma. These

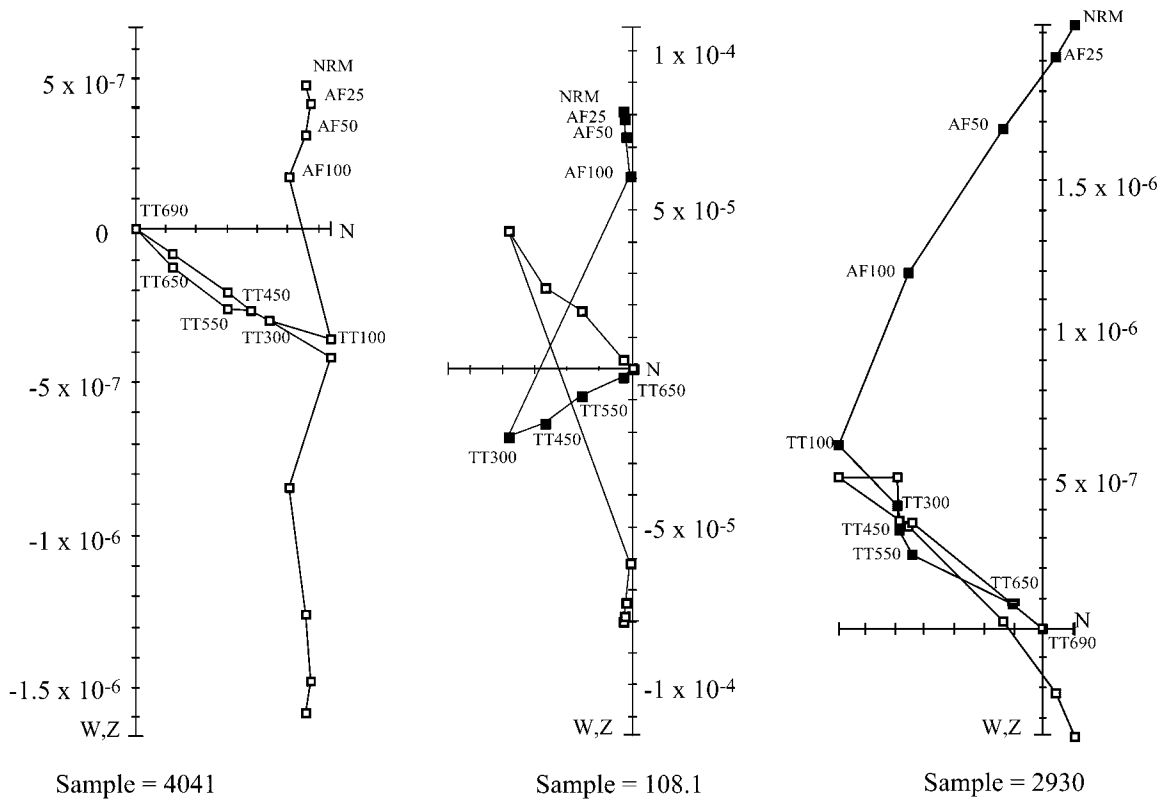


Figure 7. Plots of alternating-frequency (AF) and thermal (TD) demagnetization behavior of three representative samples from the Noruz magnetostratigraphy section. Open squares represent inclination; solid squares represent declination. Note that all three samples have both a low- and a high-coercivity component. High-coercivity components are generally stable above 300 °C.

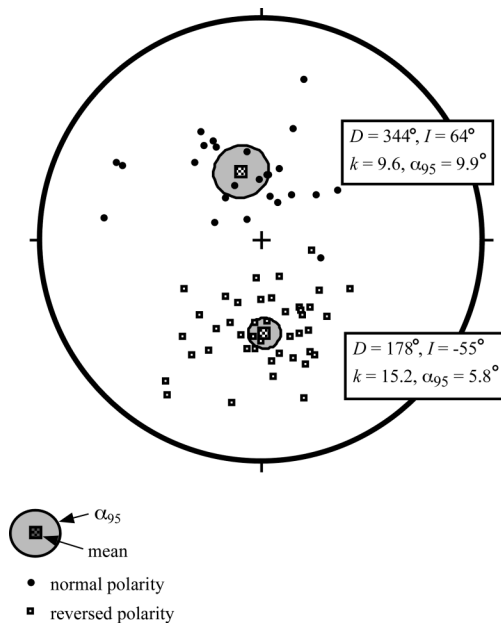


Figure 8. Normal- and reversed-site means are shown for all class I sites whose α_{95} values do not cross the 0° VGP. The data pass the C reversal test of McFadden and McElhinny (1990), suggesting that the secondary magnetic overprint was effectively removed during alternating-frequency and stepwise thermal demagnetization. D —declination, I —inclination, k — k statistic, α_{95} —radius of 95% confidence ellipse.

fossil and shell data serve to eliminate numerous alternate correlations to the GPTS.

The observed 32 magnetozones define a recognizable pattern that correlates well with chron 4Ar.2 (ca. 9.5 Ma) through chron 2An.2 (3.1 Ma) of the GPTS of Cande and Kent (1995) (Fig. 9). The top of our section (ca. 3 Ma) lies ~20 m below the base of the gray conglomerate. Without knowledge of exactly where the horse fossil (necessarily younger than 2.6 Ma) was found within the gray conglomerate, it is reasonable that the 0.5 m.y. discrepancy is accounted for in the lowermost Sharpyldak Formation. Although alternative correlations to the GPTS are possible, they require significant (unrecognized) unconformities within the section, they are inconsistent with the faunal and palynological data, or they require major changes in accumulation rates that are inconsistent with the independently derived tectonic history described in a subsequent section.

Sediment-Accumulation Rates

Following correlation with the GPTS, sediment-accumulation rates were estimated

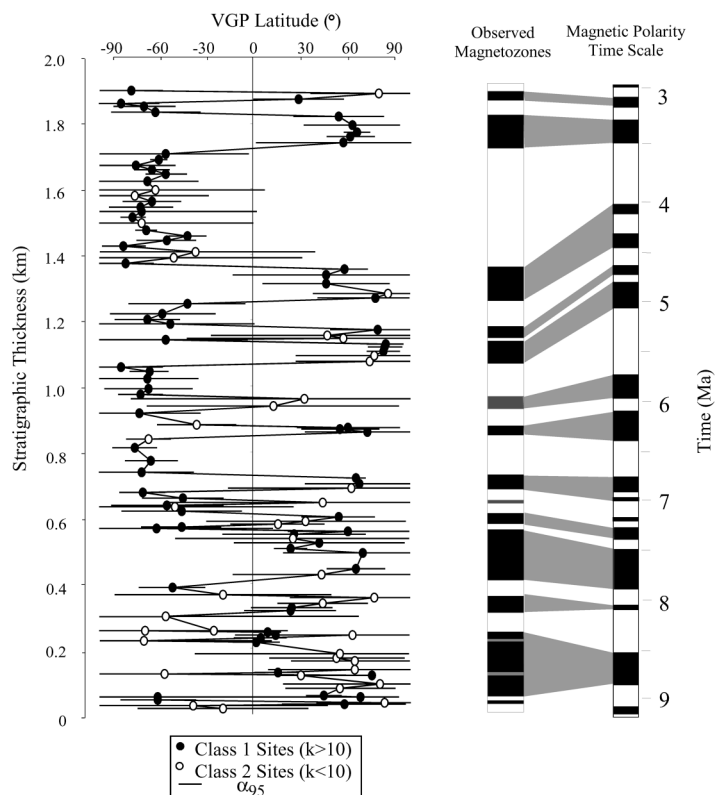


Figure 9. Magnetostratigraphy from the Noruz region correlated to the geomagnetic polarity time scale of Cande and Kent (1995). Gray magnetostratigraphic units shaded are defined by fewer than three class II sites. Boundaries between magnetostratigraphic units were defined by the midpoint between two samples with opposite polarity. α_{95} —radius of 95% confidence ellipse.

across each magnetozone (Fig. 6). Although unsteady at the 1 m.y. scale, rates of sedimentation decreased from ~ 0.38 km/m.y. before ca. 8.5 Ma to ~ 0.24 km/m.y. after 8 Ma. Following an interval of slow deposition, accumulation rates sustained a protracted increase from ca. 6 to 3 Ma. An increase in grain size and the transition from longitudinal (southeast or northwest) to transverse paleoflow (north) between ca. 6 and 3 Ma coincided with an increase in accumulation rates from <0.24 km/m.y. to ~ 0.37 km/m.y. Accumulation rates peaked at ~ 0.6 km/m.y. during braidplain deposition between 3.5 and 4 Ma. Although precise ages are not available for the upper conglomeratic (Sharpyldak) part of the Noruz section, we infer that rates of sedimentation rose well above previous levels to 0.5–1.5 km/m.y. (Fig. 6). We base this inference on the dramatic increase in grain size from the Chu Formation to the Sharpyldak Formation and the impressive thickness of the conglomeratic unit. If accumulation were slower than 0.5 km/m.y., the top of the conglomerate would be modern in age: a hypothesis that is

inconsistent with the degree of deformation and dissection of the conglomerates.

FISSION-TRACK DATING

Fission tracks are damage zones in a crystal lattice principally related to the spontaneous decay of ^{238}U . Tracks progressively shorten, or anneal, in both length and width with increasing temperature (Naeser, 1976). At temperatures of less than ~ 60 °C, tracks do not effectively shorten, whereas above 110 °C, they anneal rapidly. Between ~ 60 and 110 °C, tracks shorten in an idealized time-temperature transitional zone referred to as the partial annealing zone (PAZ). In nature, the PAZ temperature range is not fixed but is a function of cooling rate and apatite composition (Carlson et al., 1999).

Thermochronologic sampling along bedrock transects with significant topographic relief has proved useful in defining the rate and timing of exhumation (e.g., Fitzgerald et al., 1993). Fission-track ages record the time since passage through the PAZ; therefore, ages typ-

ically increase with elevation, as samples at higher elevation have spent more time at lower temperatures. Many studies have sought to identify the age versus elevation relationship characteristic of a PAZ in rocks that have been brought rapidly to the surface. Periods of very slow cooling followed by rapid cooling can preserve a break in slope in an age versus elevation plot that represents the base of the paleo-, or “exhumed” PAZ (Fitzgerald et al., 1993). The cooling age at this break in slope represents a change in erosion rate, which may reflect the initiation of tectonic activity. If the paleo-geothermal gradient is known, then the initial depth of the exhumed PAZ can be estimated and, hence, total exhumation can be calculated.

By comparison, detrital thermochronology integrates a spectrum of cooling ages from an entire drainage basin and can potentially capture an age versus elevation traverse in a single sample (Fig. 10). The difficulty, however, comes in identifying the different grain-age components that constitute a source. To isolate grain-age populations, we used a binomial peak-fitting routine that decomposes the observed age distribution into distinct component populations or peaks (Galbraith, 1988; Galbraith and Green, 1990; Brandon, 1996). The relative age of these peaks in a stratigraphic section defines the erosional evolution of the source terrane (Brandon and Vance, 1992; Garver and Brandon, 1994; Garver et al., 1999).

Analytical Procedure

Our methods for apatite separation closely follow those described by Naeser (1976) for the external detector method. A mean zeta calibration factor of 104.98 ± 5.79 (Hurford and Green, 1983) was calculated on the basis of repeated analysis of the Fish Canyon Tuff and Durango apatite age standards. Corning glass standards (CN-1) were placed at the top and bottom of the irradiated samples to monitor the fluence gradient during irradiation. When possible, more than 50 grains were dated for each of the samples collected. We only consider samples with at least 20 datable grains, because otherwise, low uranium and young ages result in very poor statistics. To test whether grain ages belong to a single component population, we employ the χ^2 test of Green (1981). The statistical validity of each component population is represented by the width of the peak, which is a function of the standard deviation and total number of dated grains. All standard deviations are reported here at the $\pm 1\sigma$ level. Because of the diffi-

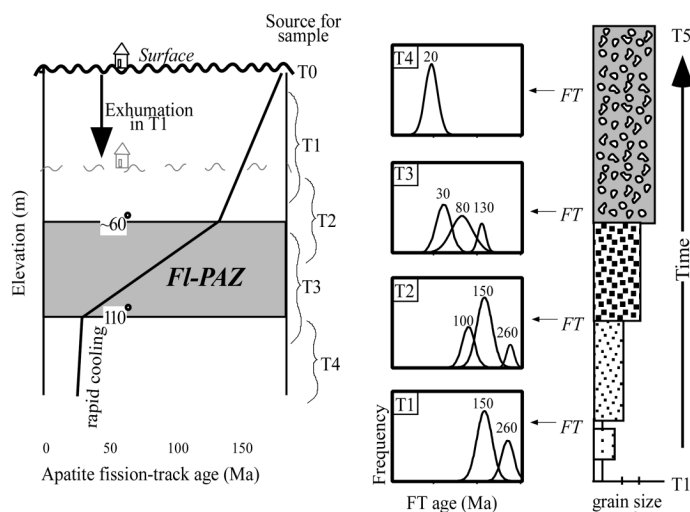


Figure 10. Model for detrital signature of progressive unroofing (at times T1 to T4) through a crustal column, which preserves an exhumed apatite partial annealing zone (PAZ). Erosion of a source results in the inverse age stratigraphy in an adjacent basin (after O'Sullivan and Parrish, 1995). FT—fission track.

culties in isolating component populations, some workers (Hendrix et al., 1994; Sobel and Dumitru, 1997) have opted to propagate a $\pm 1\sigma$ uncertainty of 15% error. Although we do not follow this method, we conservatively fit the smallest number of peaks to each observed population.

Bedrock Fission-Track Ages

Apatite fission-track and [U-Th]/He (He) dates from a sampling transect of 2.4 km relief in the Ala Archa drainage, located 27 km west of the Noruz section (Fig. 2), place independent bounds on the cooling history of the Kyrgyz Range (Figs. 11 and 12) (Bullen, 1999). The most significant feature of these data is the break in slope of the fission-track age versus elevation data at ca. 11 Ma. This break is interpreted as the base of an exhumed PAZ, representing the initiation of exhumation in the Kyrgyz Range. From these thermochronologic data, Bullen (1999) interpreted the following scenario: (1) between ca. 103 Ma and 11 Ma, the Kyrgyz Range was tectonically quiescent (exhumation rates $< \sim 0.05$ km/m.y.); (2) rapid exhumation (~ 1.5 km/m.y.) of the northern Tien Shan began at ca. 11 Ma and continued for 1–1.5 m.y.; (3) erosion rates decreased to < 0.3 km/m.y. between 10 Ma and 3 Ma; and (4) exhumation rates accelerated at ca. 3 Ma to 0.8 km/m.y. (Fig. 12). By assuming that the present-day geothermal gradient of 26 °C/km is similar to that since 11 Ma, Bullen (1999) calculated a total of ~ 6 km

of rock uplift, 4 km of exhumation, and ~ 2 km of surface uplift.

Detrital Fission-Track Stratigraphy

Four sandstones with depositional ages of 8.5 Ma, 4.5 Ma, 2.5–2 Ma, and ca. 1.5–1 Ma (Fig. 6) were collected for fission-track analysis from the Noruz section. As expected, all samples exhibit wide ranges of cooling ages and therefore fail the χ^2 test, attesting to a heterogeneous source without significant post-depositional heating (Table 1). After separating best-fit component peaks for each observed grain-age population (Table 1), it is clear that young peak ages (P1) decrease upward through the section from 165 ± 14 Ma at the base to 15 ± 4 Ma at the top (Fig. 6), whereas the proportion of grains that constitute the older peaks (P2 and P3) of ca. 150, 260, and 471 Ma decreases.

Interpretation

Our peak-fitting results document both a young moving peak and an older, poorly defined moving peak (Figs. 6 and 13). We interpret that this progression in grain ages records unroofing of a crustal column that contained three thermotectonic layers: (1) heterogeneous older rocks that resided above the PAZ (Jurassic and older), (2) intermediate age rocks from within the exhumed PAZ (early Tertiary–Cretaceous), and finally (3) fully reset rocks from below or just at the base of the PAZ

(Tertiary). We interpret these three age layers to correspond with crustal zones containing component populations of > 150 Ma, 80–55 Ma, and 20–10 Ma, respectively (Fig. 13, Table 1). Despite the range of ages, the reconstructed age layers add considerable detail to the age versus elevation profile documented by Bullen (1999), but most importantly, they provide independent confirmation of the preservation of an exhumed, or relict, apatite PAZ in the Kyrgyz Range.

By knowing the depositional age of sandstones used for detrital fission-track analysis, we are able to estimate the time at which certain age populations appeared in the Chu basin. If we assume that the transit time between the hinterland and foreland basin is minimal, then we can also approximate when different age layers were exposed at the surface in the Kyrgyz Range. In our detrital record, exposure of the apatite PAZ is recorded by the appearance of a 56 ± 7 Ma grain-age population by 4.5 Ma. In a similar manner, the influx of < 15 Ma grains at ca. 1.5 Ma implies that rocks from below the PAZ (4–5 km depth) were at the surface by this time. It is also interesting that the young peak ages change little between 4.5 and ca. 2 Ma (56 ± 7 and 51 ± 5 Ma, respectively), suggesting that either (1) the same source was being eroded and hence erosion was minimal or (2) there was rapid cooling at ca. 55 Ma and the thermotectonic layer is relatively thick. The depositional record of this area offers no support for an Eocene exhumation event (Chediya et al., 1973), during an interval otherwise characterized by soil formation and slow carbonate deposition associated with the Kokturpak Formation. If the slow exhumation rates in the Kyrgyz Range between 10 and 3 Ma (Bullen, 1999) are considered, it seems more likely that the same source rocks were preserved near the surface between 4.5 and ca. 2 Ma during an interval of relatively slower erosion.

Late Jurassic (165 ± 13 Ma) fission-track ages constitute the main population in the lowest detrital sample (Fig. 6) and are the consequence of erosion of old, shallow crust during the initial stages of uplift and exhumation. This homogeneous-age population allows us to improve upon the estimates from bedrock thermochronology (Bullen, 1999) to state that (1) the last regional cooling event occurred in the Late Jurassic and (2) the average exhumation rate between 165 and 11 Ma was very slow (< 0.035 km/m.y.). There are also two older cooling events apparent from these data: one in the Permian (ca. 270 Ma) and one in the Middle Ordovician (471 Ma). Persistence of these Permian and Ordovician ages indi-

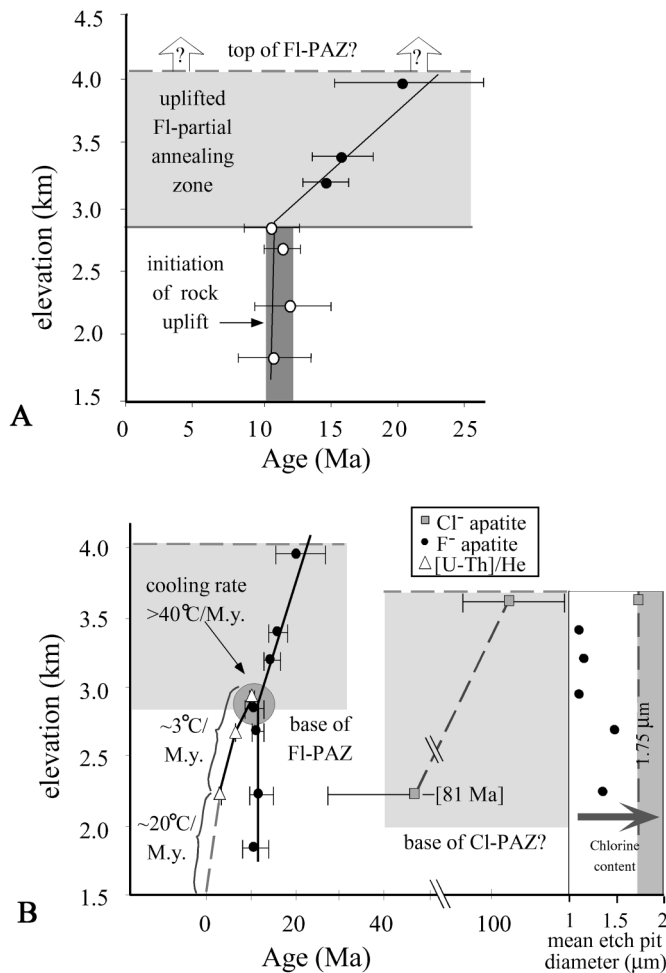


Figure 11. Bedrock age data from the Kyrgyz Range (from Bullen, 1999). (A) Fission-track data from a sampling transect of 2.4 km relief demonstrate the Kyrgyz Range, northern Tien Shan. A sample with an anomalously old age of 103 Ma was excluded from this plot. (B) Fission-track and (U-Th)/He ages from the sampling transect. Two fission-track samples are interpreted as containing chlorapatite. The sample from 3.6 km shows the increased etch-pit diameter associated with chlorapatite, whereas the sample from 2.2 km fails the χ^2 test and has two component age populations, one at ca. 12 Ma and another at ca. 80 Ma. This older population of ages is interpreted to represent chlorapatite grains. Chlorapatites have a higher annealing temperature ($\sim 150^\circ\text{C}$). The 103 Ma age of the chlorapatite sample at 3.6 km indicates that cooling between 100 Ma and 20 Ma occurred at rates of $\sim 0.5^\circ\text{C}/\text{m.y.}$ This cooling rate indicates that erosion of the hinterland was very slow prior to 11 Ma. The similarity in He and fission-track ages at ~ 2.8 km reflects a rapid cooling event between 11 and 10 Ma. Cooling rates decreased between 10 and 3 Ma, as shown by the shallow age vs. elevation gradient. Cooling rates accelerated at 3 Ma to $\sim 25^\circ\text{C}/\text{m.y.}$ FI-PAZ—fluorapatite partial annealing zone, Cl-PAZ—chlorapatite partial annealing zone.

icates that the total exhumation during the Jurassic was minimal ($<2\text{--}3$ km).

Fission-Track Dating of Modern River Sediment

Sand from two modern rivers was collected ~ 76 km apart along the northern flank of the

Kyrgyz Range (Figs. 2 and 14). The character of the Kyrgyz Range changes significantly along strike. The width of the range, as defined by the distance from drainage divide to the northernmost exposed bedrock, decreases by a factor of two from Ala Archa (34 km width) to near the Shamsi River (14 km width). Maximum summit heights in the head-

waters of the Shamsi catchment are typically less than 4000 m, whereas those in the Ala Archa region are as high as 4850 m. Additionally, the Shamsi River effectively marks an important structural transition, in that the dominant structural vergence changes from north (near Ala Archa) to south (east of Shamsi River).

The sample at the mouth of the Ala Archa drainage comprises sand from the same drainage where the apatite fission-track transect of Bullen (1999) was collected (Fig. 2). Two component populations of 17 ± 2 and 78 ± 2 Ma were statistically separated in this sample (Fig. 14; Table 1). A second sample of river sediment was collected 76 km to the east along the Shamsi River (Fig. 2) in order to improve our understanding of the spatial development of the Kyrgyz Range. This sample has three component populations (Fig. 14) of 11 ± 3 , 68 ± 5 , and 149 ± 12 Ma (see Table 1).

Interpretation

Fission-track ages from the Ala Archa and Shamsi Rivers are best understood in the context of the detrital fission-track samples from the Noruz section (Figs. 6, 11, 14). In these samples, the decrease in peak ages upward in the section records unroofing of a crustal column with distinct age layers (Figs. 10 and 13). Following this model, the sample from the Ala Archa River, with peak ages of 17 ± 2 and 78 ± 9 Ma (Fig. 14), documents exposure and erosion of rocks that resided within and beneath the base of an exhumed apatite PAZ. The sample from the Shamsi drainage area is composed predominantly of grains that sat within and above the apatite PAZ. The low percentage of grains ($\sim 5\%$) that define the young peak of 11 Ma in the Shamsi River sample suggests that only a small amount of fully reset rocks are currently exposed at the surface. Given the older detrital ages, narrower range width, and lower summit elevations in the eastern section of the Kyrgyz Range, it seems likely that the Shamsi region has undergone significantly less exhumation than the Ala Archa region. This finding may be a function of either variable rates of exhumation or eastward propagation of the Kyrgyz Range.

TECTONIC SYNTHESIS

We propose a four-stage tectonic model for the northern Tien Shan that involves two periods of rapid exhumation and relates the depositional record to widely cited models for foreland basins (Fig. 15).

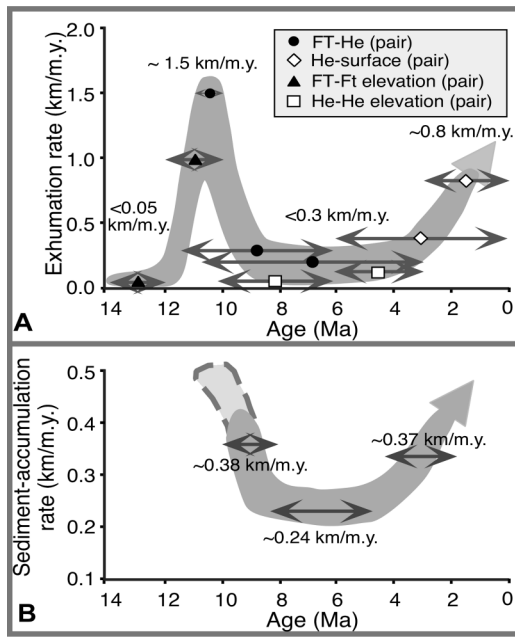


Figure 12. (A) Exhumation rates from 14 Ma to the present in the Kyrgyz Range, reconstructed from pairs of thermochronologic data (from Bullen, 1999). Horizontal arrows represent the duration of the calculated exhumation rate. (B) Sediment-accumulation rates in the Chu foreland basin based on magnetostratigraphic data. Dashed region indicates estimated rates based on strata preserved beneath the dated section.

1. Fission-track thermochronology indicates that the northern Tien Shan was tectonically quiescent between 165 and 11 Ma. However, both drill-hole and outcrop data reveal that ~0.6 km of Cretaceous–Paleogene (and perhaps lower Miocene) strata were deposited prior to 11 Ma (Fig. 16A). As these older strata predate uplift of the Kyrgyz Range, we in-

terpret that they represent a distal facies derived from contemporaneous uplift in the central and/or eastern Tien Shan.

2. Bedrock cooling ages indicate rapid exhumation of ~1.5 km in the Kyrgyz Range between 11 and 10 Ma (Fig. 16B) (Bullen, 1999). Because our record of deposition in the Chu basin extends only to 9 Ma (base of the

magnetostratigraphy section), we have no data with which to interpret the synorogenic depositional setting or sedimentation rates. However, well-log data (Chediya et al., 1973) indicate ~2–3 km of fluviolacustrine Neogene sedimentary deposits beneath the base of the Noruz section (Fig. 5). The upper part of this sequence is likely a repetition of the exposed Noruz section in the hanging wall of the Issyk Ata fault (Fig. 5), but the remaining strata probably comprise both the preorogenic Cretaceous–Paleogene (lower Miocene?) Kokturpak and Kokmeren Formations and, more important, upper Miocene deposits associated with initiation of exhumation in the Kyrgyz Range. Given the duration of the exhumation pulse at 11 Ma, the synorogenic sediment probably accumulated at rates exceeding 0.5 km/m.y. (Fig. 12).

We propose that accelerated loading by the Kyrgyz Range trapped conglomeratic strata proximal to the thrust front, ~10–15 km south of the Noruz section (Fig. 15B) (Beck et al., 1988; Heller et al., 1988). In this regard, we propose that the Noruz section was positioned in a medial to distal position within the foreland with respect to the Kyrgyz Range during range initiation at 11 Ma. The playa deposition that persisted until ca. 8.5 Ma is indicative of conditions in which subsidence outpaced sediment supply (Beck et al., 1988). We additionally suggest that fine-grained detritus was supplied to the Chu basin as the Cretaceous–Paleogene strata were stripped off the Kyrgyz Range. If this is the case, lithologic characteristics of the source area controlled the nature of deposition in the adjacent foreland (Fig. 15C) (DeCelles et al., 1991). Detrital fission-track ages indicate that the total exhumation in the Kyrgyz Range was minor (<1–2 km) at this time (top panel, Fig. 14).

3. Accumulation rates in the Chu basin decelerated to ~0.24 km/m.y. between 8 and 5 Ma, corresponding notably with slower exhumation rates of <0.3 km/m.y. in the Kyrgyz Range (Bullen, 1999) (Fig. 12). To the extent resolvable with the available time control, these changes in exhumation and sediment-accumulation rates were synchronous (Fig. 12). Despite decreased rates of sediment accumulation after 8 Ma, mean grain size steadily increased during the subsequent 5 m.y. Models of foreland-basin deposition suggest that when thrust loading is slower, erosion and subsequent isostatic rebound of the hinterland can result in dispersal of coarse-grained sediments into the foreland (Fig. 15B) (Heller et al., 1988; Beck et al., 1988; Burbank, 1992). Whereas rates of exhumation, and probably also thrust loading, were slower between 8

TABLE 1. FISSION-TRACK RESULTS FROM THE DETRITAL SEQUENCE SHED FROM NORTHERN TIEN SHAN

Sample	Strat. height (m)	Number of grains	Depositional age (Ma)	Peak 1 (Ma)	Peak 2 (Ma)	Peak 3 (Ma)	Peak 4 (Ma)	Peak 5 (Ma)
6	MS (Shamsi)	86	0	11 ± 3 $\pi_1 = 5\%$ $W = 0.59$	68 ± 5 $\pi_1 = 37\%$ $W = 0.31$	149 ± 12 $\pi_1 = 58\%$ $W = 0.37$		
5	MS (Ala Archa)	83	0	17 ± 2 $\pi_1 = 64\%$ $W = 0.72$	78 ± 2 $\pi_1 = 36\%$ $W = 0.53$			
4	2900	20	ca. 1	15 ± 4 $\pi_1 = 46\%$ $W = 0.58$	25 ± 6 $\pi_1 = 49\%$ $W = 0.49$		321 ± 180 $\pi_1 = 5\%$ $W = 0.062$	
3	2500	38	ca. 2		51 ± 5 $\pi_1 = 37\%$ $W = 0.33$		233 ± 18 $\pi_1 = 45\%$ $W = 0.25$	471 ± 65 $\pi_1 = 18\%$ $W = 0.32$
2	1230	40	4.5		56 ± 7 $\pi_1 = 49\%$ $W = 0.42$	149 ± 17 $\pi_1 = 51\%$ $W = 0.41$		
1	212	67	9.8			165 ± 13 $\pi_1 = 79\%$ $W = 0.33$	264 ± 47 $\pi_1 = 21\%$ $W = 0.36$	

Note: Peak ages are found by using the binomial peak-fitting method of Galbraith (1988) and Galbraith and Green (1990), from a routine written by Brandon (1996). All peak-age errors are reported at the 1 σ level. In peak columns, π_1 is proportion of grains that compose a peak, and W is relative width of the binomial peak as a proportion of its age.

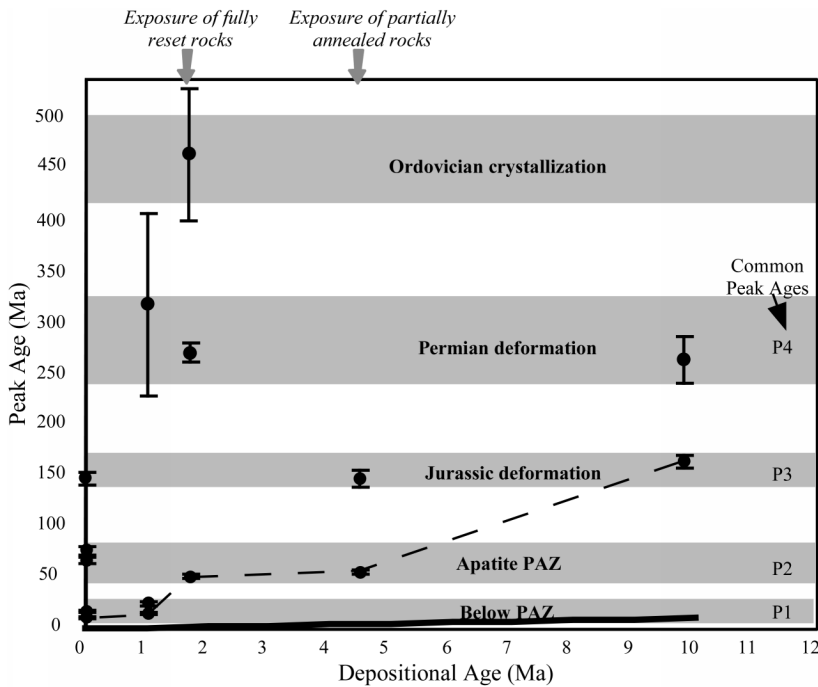


Figure 13. Depositional age vs. peak age for detrital fission-track samples. We recognized four “common” peaks in these samples, at ca. 260, 150, 55–80, and 20–10 Ma. Solid line represents the 1 to 1 line. Dashed line connects the youngest peak ages to emphasize the progressive exposure of deeper-crustal levels. Lag times are shown in square brackets.

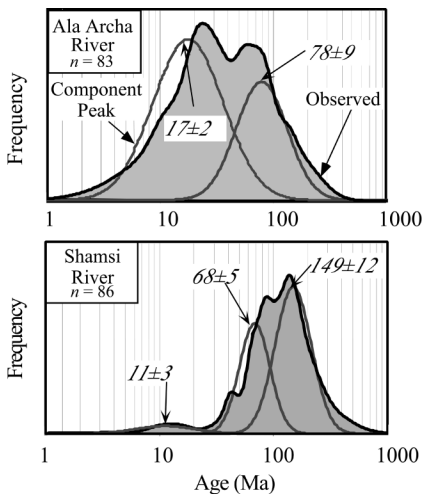


Figure 14. Grain-age distributions from two modern stream samples along the Kyrgyz Range. The Shamsi River is transporting predominantly Jurassic–Cretaceous grains, suggesting that an exhumed PAZ had just recently been exposed. In contrast, fully reset and partially reset grains compose the Ala Archa stream sample, which indicates that rocks from below the PAZ (>4 km depth) are just now being exposed at the surface.

and 5 Ma (Fig. 12), the deformation front still advanced into the foreland, and the bedrock source area was therefore in a more proximal position (Fig. 15A). Additionally, by ca. 8 Ma, Cenozoic strata would have been stripped off the Paleozoic rocks of the central Kyrgyz Range, exposing more resistant lithologies (e.g., Ordovician granite) that would contribute to the upward-coarsening sequence (Fig. 15C). Therefore, we interpret the upward-coarsening trend to be due to a combination of (1) isostatic rebound of the Kyrgyz Range, (2) encroachment of the thrust front, and/or (3) increased availability of resistant lithologies in the source area.

4. Shortening occurred along the Issyk Ata fault as deformation propagated into the Chu basin at 3–2 Ma (Fig. 16D). There is a clear temporal and structural link between thrusting along the Issyk Ata fault, rock uplift in the hinterland, and influx of conglomerates into the foreland, irrespective of any climatic influences on rates of erosion or the production of conglomerates (Figs. 12 and 16) (Molnar and England, 1990). Rates of conglomerate accumulation accelerated to >0.5 km/m.y. in the Sharpyldak Formation, significantly exceeding those in the underlying Chu Formation. As the Issyk Ata fault propagated into the foreland, it created a piggyback basin on its hanging

wall that acted as a trap to conglomeratic influx.

CONCLUSIONS

The preceding analysis provides new insights on the timing and character of deformation in the northern Tien Shan. The value of such a synthesis is emphasized by considering the likely interpretation of each method independently. If the detrital fission-track signature were evaluated alone, one might conclude that uplift commenced at ca. 4.5 Ma, which is the first time there is a clear indication that rocks from within the apatite partial annealing zone (PAZ) were exposed at the surface (Fig. 6). On the basis of classic interpretations of the relationship of thrusting to conglomerate deposition (Fig. 15A), deformation would be defined as beginning at ca. 5 Ma, when conglomerates became more abundant. In contrast, our data indicate that there may be a significant temporal lag (5–7 m.y.) between the initiation of rock uplift and the influx of conglomerates to a site within the adjacent foreland. It is therefore clear that reliance on any one approach could lead to significant misinterpretations. Nonetheless, even after combining a well-defined erosional history of the hinterland with accumulation rates and detrital ages in the adjacent foreland, our proposed tectonic model is, at some level, incomplete. A detailed study of climate change in the region could augment or improve upon our interpretations regarding sediment accumulation and hinterland exhumation. Likewise, additional petrographic and thermochronologic analysis in the Chu basin would help eliminate the multiple hypotheses concerning range propagation, thrust loading and basin subsidence, and source lithology.

Detrital fission-track ages from the Noruz section document unroofing of a crustal column that contained three thermotectonic layers represented by ages older than 150 Ma, 80–55 Ma, and 20–10 Ma (Fig. 13, Table 1). These age layers add detail to the age versus elevation profile documented by Bullen (1999) and provide independent confirmation of the preservation of an exhumed apatite PAZ in the Kyrgyz Range. Bedrock fission-track ages (Bullen, 1999) demonstrate that exhumation and deformation in the Kyrgyz Range was complex after 11 Ma, with at least four intervals defined by changes in exhumation rate. Rates of deposition in the foreland are generally synchronous with changes in erosion rates and inferred deformation in the hinterland.

Fission-track data from modern river sedi-

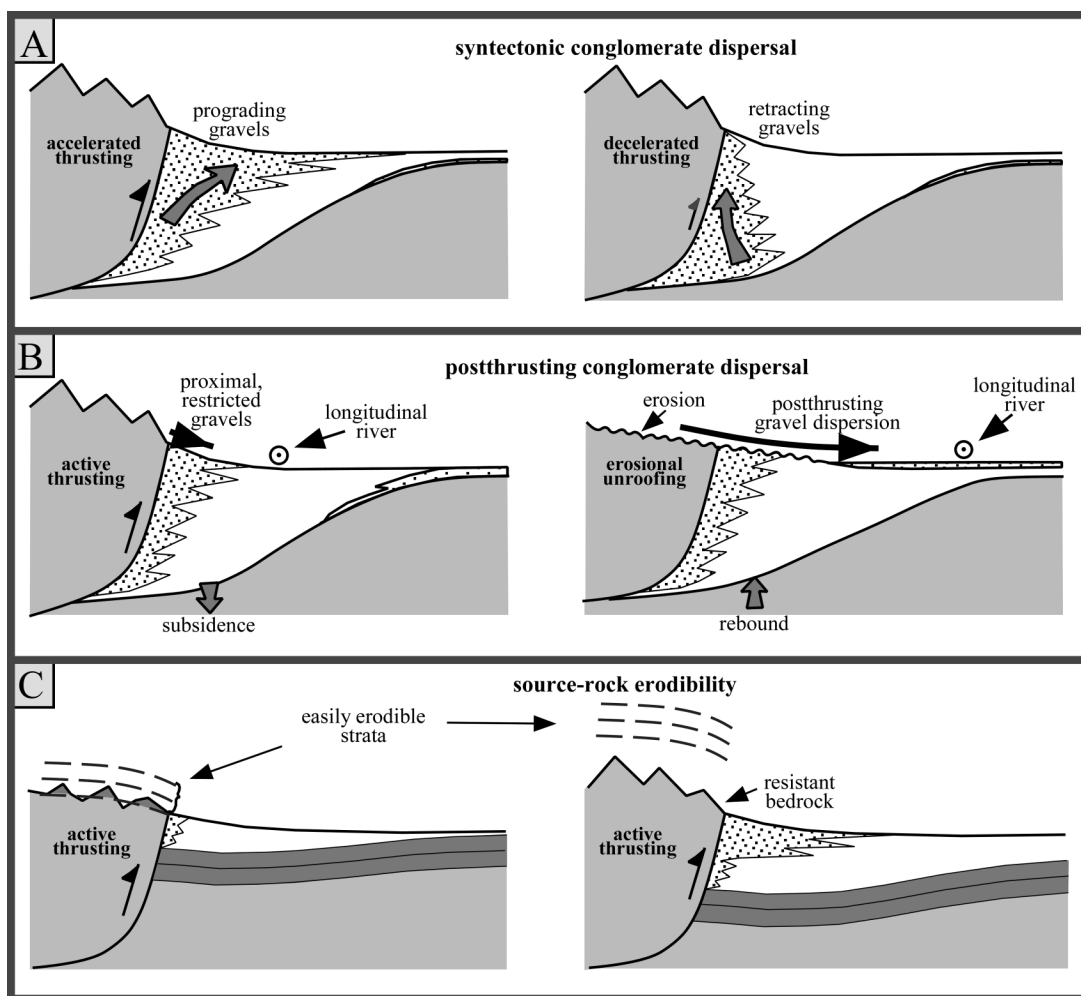


Figure 15. Conceptual models depicting the depositional response to variable tectonic activity. (A) The “classical model” predicts that coarse-grained sediments will prograde extensively into a flexural foreland coincident with significant thrusting events. (B) Flexural model of Heller et al. (1988) proposes that coarse detritus will be trapped in the zone of maximum subsidence during thrust-belt activity. Erosion dominates during the postthrusting interval, resulting in flexural rebound of the thrust belt and conglomerate dispersal into the basin center. (C) Source-rock erodibility exerts a strong control on the grain-size distribution of the eroded sediments. Erosion of weakly lithified strata occurs rapidly, thereby decreasing the creation of accommodation space and providing the basin with primarily fine-grained sediments.

ments indicate that the magnitude of erosion in the hinterland is considerably greater in the western Kyrgyz Range than it is in the east. In addition, differences in mean elevation, width of the range, and degree of preservation of the pre-Cenozoic unconformity indicate that more deformation has occurred in the western Kyrgyz Range. For these reasons, we propose that deformation has propagated from west to east along the range.

If previous estimates of late Oligocene to early Miocene initiation of deformation along the southern and eastern margins of the Tien Shan are correct (Hendrix et al., 1994; Sobel and Dumitru, 1997; Yin et al., 1998), then deformation progressively advanced from south to north and from east to west. Our data indicate that deformation did not begin in the

Kyrgyz Range prior to the late Miocene. Widespread Cretaceous–Paleogene (lower Miocene?) strata mantling the Kyrgyz Range is consistent with tectonic quiescence across this region. Additionally, pre-Cretaceous detrital fission-track ages from 9 Ma strata indicate that erosion of the Paleozoic bedrock was minimal at this time.

Finally, on the basis of these data, the causal relationship, if any, between uplift of the Tibetan Plateau and development of the Tien Shan remains unclear. Rapid rise of the Tibetan Plateau at ca. 8 Ma could have increased the horizontal force transmitted to central Asia and hence may have been the catalyst for late Miocene shortening within the Tien Shan (Molnar et al., 1993). However, given the temporal discrepancy between the time of initia-

tion of deformation in the northern Tien Shan (11 Ma) and the interpreted time of maximum uplift of Tibet (8 Ma), either the two events are not directly related or the rise of the plateau was protracted.

ACKNOWLEDGMENTS

We are greatly indebted to J. Lave, S. Thompson, R. Weldon, K. Mclean, E. Sobel, and M. Miller for risking life and limb to collect paleomagnetic samples. We thank Joseph Kirschvink of the California Institute of Technology for the use of his paleomagnetic lab facilities and helpful advice. We also appreciate help from Ray Bernor and Alan Walker with vertebrate fossil identification. The stereonet program of Rick Allmendinger was used in this study. Steve Binney, director of the Oregon State Nuclear reactor, expedited sample irradiation. This project was supported by grants from the National

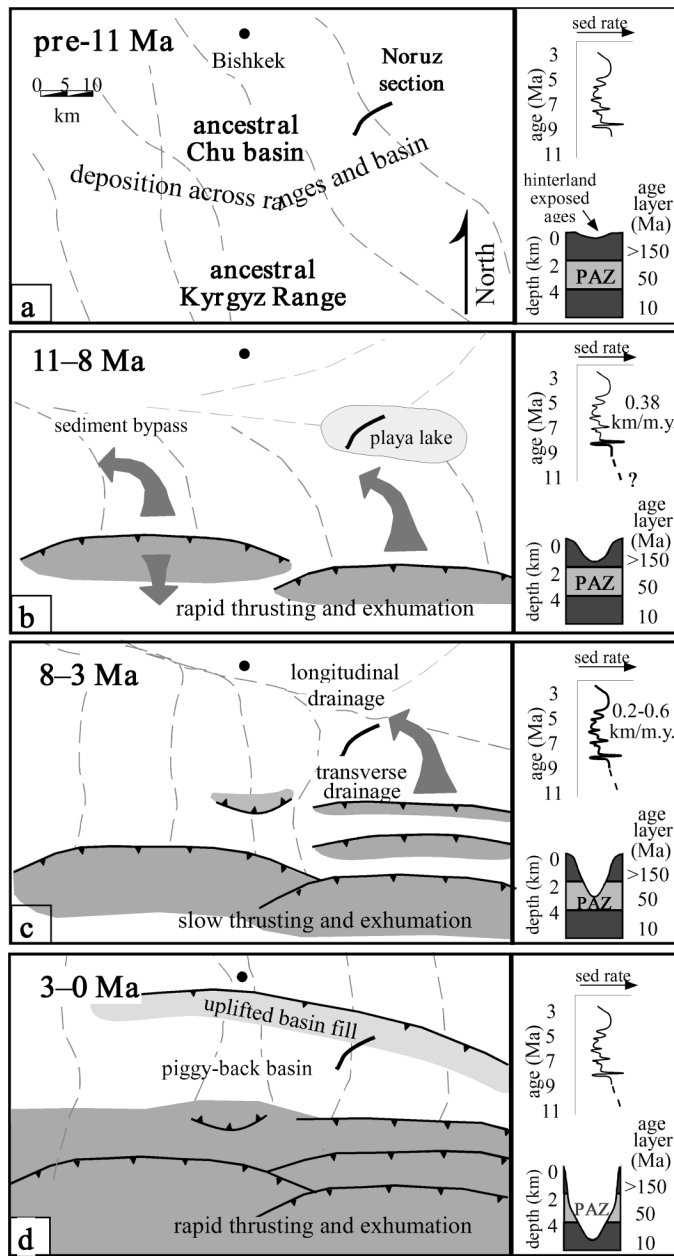


Figure 16. Schematic model for the Cenozoic tectonic evolution of the northern Tien Shan. Panels on the right depict the sediment-accumulation rate (sed rate) in the Chu basin (top), for each time interval (heavy line). The extent of exhumation and the exposed fission-track ages in the Kyrgyz Range are shown in an idealized crustal column for each time interval (at the bottom of each panel on the right).

Science Foundation (EAR 96-4765; Continental Dynamics) and the National Aeronautics and Space Administration (NAG-7646) and by a fellowship from Anadarko Petroleum. We thank R. Slingerland, D. Fisher, A. Yin, M. Hendrix, and P. Copeland for thoughtful reviews.

REFERENCES CITED

Abdrakhmatov, K.Y., Aldazhanov, S.A., Hager, B.H., Hamburger, M.W., Herring, T.A., Kalabaev, K.B., Maka-

rov, V.I., Molnar, P., Panasyuk, S.V., Prilepin, M.T., Reilinger, R.E., Sadybakasov, I.S., Souter, B.J., Trapeznikov, Y.A., Tsurkov, V.Y., and Zubovich, A.V., 1996, Relatively recent construction of the Tien Shan inferred from GPS measurements of present-day crustal deformation rates: *Nature*, v. 384, p. 450-453.
 Allen, M.B., Windley, B.F., and Zhang Chi, 1992, Palaeozoic collisional tectonics and magmatism of the Chinese Tien Shan, *Central Asia: Tectonophysics*, v. 220, p. 89-115.
 Allen, M.B., Windley, B.F., Zhang Chi, and Guo Jinghui, 1993, Evolution of the Turfan Basin, *Chinese Central Asia: Tectonics*, v. 12, p. 889-896.

Atlas Kyrgyzskoi CCP I, 1987: Moscow, Academia Nauk Kyrgyzskoi CCP, p. 1-157.
 Avouac, J.P., Tapponnier, P., Bai, M., You, H., and Wang, G., 1993, Active thrusting and folding along the northern Tien Shan and late Cenozoic rotation of the Tarim relative to Dzungaria and Kazakhstan: *Journal of Geophysical Research*, B, Solid Earth and Planets, v. 98, p. 6755-6804.
 Bally, A.W., Ming Chou, I., Clayton, R., Heugster, H.P., Kidwell, S., Meckel, L.D., Ryder, R.T., Watts, A.B., and Wilson, A.A., 1986, Notes on sedimentary basins in China, in Report of the American sedimentary basins delegate to the People's Republic of China, August 17-September 8, 1985: U.S. Geological Survey Open-File Report 86-327, p. 108.
 Beck, R.A., Vondra, C.F., Filkins, J.E., and Olander, J.D., 1988, Syntectonic sedimentation and Laramide basement thrusting, Cordilleran foreland; Timing of deformation, in Schmidt, C.J., and Perry, W.J., Jr., eds., Interaction of the Rocky Mountain foreland and the Cordilleran thrust belt: *Geological Society of America Memoir* 171, p. 465-487.
 Bentham, P.A., Talling, P.J., and Burbank, D.W., 1993, Braided stream and flood-plain deposition in a rapidly aggrading basin: The Escanilla Formation, Spanish Pyrenees, in Best, J.L., and Bristow, C.S., eds., Braided rivers: *Geological Society of London Special Publication* 75, p. 177-194.
 Brandon, M.T., 1996, Probability density plot for fission-track grain-age samples: *Radiation Measurements*, v. 26, p. 663-676.
 Brandon, M.T., and Vance, J.A., 1992, Fission-track ages of detrital zircon grains: Implications for the tectonic evolution of the Cenozoic Olympic subduction complex: *American Journal of Science*, v. 292, p. 565-636.
 Bridge, J.S., and Leeder, M.R., 1979, A simulation model of alluvial stratigraphy: *Sedimentology*, v. 26, p. 617-644.
 Brown, E.T., Bourles, D.L., Burchfiel, B.C., Deng Qidong, Li Jun, Molnar, P., Raisbeck, G.M., and Yiou, F., 1998, Estimation of slip rates in the southern Tien Shan using cosmic ray exposure dates of abandoned alluvial fans: *Geological Society of America Bulletin*, v. 110, p. 377-386.
 Bullen, M.E., 1999, Late Cenozoic tectonic evolution of the Kyrgyz Range and adjoining Chu basin: New age constraints from fission-track, (U-TH)/HE, and magnetostratigraphy [M.S. thesis]: University Park, Pennsylvania State University, 116 p.
 Burbank, D.W., 1992, Causes of recent Himalayan uplift deduced from deposited patterns in the Ganges basin: *Nature*, v. 357, p. 680-683.
 Burbank, D.W., and Reynolds, R.G.H., 1988, Stratigraphic keys to the timing of thrusting in terrestrial foreland basins: Applications to the northwestern Himalaya, in Kleinspehn, K.L., and Paola, C., eds., *New perspectives in basin analysis*: New York, Springer-Verlag, p. 332-351.
 Burtman, V.S., 1975, Structural geology of the Variscan Tien Shan: *American Journal of Science*, v. 280, p. 725-744.
 Burtman, V.S., 1980, Faults of middle Asia: *American Journal of Science*, v. 275A, p. 157-186.
 Burtman, V.S., Skobelev, S.F., and Molnar, P., 1996, Late Cenozoic slip on the Talas-Ferghana fault, the Tien Shan, Central Asia: *Geological Society of America Bulletin*, v. 108, p. 1004-1021.
 Cande, S.C., and Kent, D.V., 1995, Revised calibration of the geomagnetic polarity timescale for the Late Cretaceous and Cenozoic: *Journal of Geophysical Research*, v. 100B, p. 6093-6095.
 Carlson, W.D., Donelick, R.A., and Ketcham, R.A., 1999, Variability of apatite fission-track annealing kinetics I: Experimental results: *American Mineralogist*, v. 84, p. 1213-1223.
 Carroll, A.R., Graham, S.A., Hendrix, M.S., Ying, D., Zhou, D., 1995, Late Paleozoic tectonic amalgamation of northwestern China: Sedimentary record of the northern Tarim, northwestern Turpan, and southern Junggar basins: *Geological Society of America Bulletin*, v. 107, p. 571-594.

- Chediya, O.K., Yazovskii, V.M., and Fortuna, A.B., 1973, O stratigraficheskom raschlenenii krasnotsvetnogo kompleksa v Chuyskoy vpadine I yeye gornom obramlenii [The stratigraphic subdivision of the Kyrgyz red-bed complex in the Chu Basin and the surrounding mountains], in Chediya, O.K., ed., Zakonomernosti geologicheskogo razvitiya Tyan-Shanya v kaynozoye [Principles of the geologic development of the Tyan-Shan in the Cenozoic]: Bishkek, Ilim Press, p. 26–52.
- Chediya, O.K., Abdрахmatov, K.Ye., Lamzin, I.H., Michel, G., and Michailov, V., 1998, Seismotectonic characterization of the Issyk Ata fault: Bishkek, Institute Nauk Kyrgyzskoi, p. 58–69.
- DeCelles, P., Gray, M.B., Ridgway, K.D., Cole, R.B., Srivastava, P., Pequera, N., and Pivnik, D.A., 1991, Kinematic history of a foreland basin uplift from Paleogene synorogenic conglomerate, Beartooth Range, Wyoming and Montana: Geological Society of America Bulletin, v. 103, p. 1458–1475.
- Fisher, R.A., 1953, Dispersion on a sphere: Proceedings of the Royal Society of London, v. A217, p. 295–305.
- Fitzgerald, P.G., Stump, E., and Redfield, T.F., 1993, Late Cenozoic uplift of Denali and its relation to relative plate motion and fault morphology: Science, v. 259, p. 497–499.
- Flemings, P.B., and Jordan, T.E., 1989, A synthetic stratigraphic model of foreland basin development: Journal of Geophysical Research, v. 94B, p. 3851–3866.
- Fortuna, A.V., 1973, Palynological characteristics of the Sharpyldak Formation in the Chu Basin: Bishkek, Ilim Press, p. 41–49.
- Galbraith, R.F., 1988, Graphic display of estimates having different standard errors: Technometrics, v. 30, p. 271–281.
- Galbraith, R.F., and Green, P.F., 1990, Estimating the component ages in a finite mixture: Nuclear Tracks Radiation Measurements, v. 17, p. 197–206.
- Garver, J.I., and Brandon, M.T., 1994, Erosional exhumation of the British Columbia Coast Ranges as determined from fission-track ages of detrital zircon from the Tofino basin, Olympic Peninsula, Washington: Geological Society of America Bulletin, v. 106, p. 1398–1412.
- Garver, J.I., Brandon, M.T., Roden-Tice, M., and Kamp, P.J.J., 1999, Erosional exhumation determined by fission-track ages of detrital apatite and zircon, in Ring, U., Brandon, M.T., Lister, G.S., and Willett, S.D., eds., Exhumation processes: Normal faulting, ductile flow, and erosion: Geological Society of London Special Publication 154, p. 283–304.
- Ghose, S., Mellors, R.J., Korjenkov, A.M., Hamburger, M.W., Pavlis, T.L., Pavlis, G.L., Omuraliev, M., Mamyrov, E., and Muraliev, A.R., 1997, The $M_s = 7.3$ 1992 Suusamy, Kyrgyzstan, earthquake in the Tien Shan; 2. Aftershock focal mechanisms and surface deformation: Bulletin of the Seismological Society of America, v. 87, p. 23–38.
- Green, P.F., 1981, A new look at statistics in fission-track dating: Nuclear Tracks Radiation Measurements, v. 5, p. 77–86.
- Hao, Y.C., and Zeng, X.L., 1984, Discussion of the Mesozoic–Cenozoic evolution of the western Tarim basin based on foraminifera: Chinese Micropaleontological Bulletin, v. 1, p. 1–4.
- Heller, P.L., Angevine, C.L., Winslow, N.S., and Paola, C., 1988, Two-phase stratigraphic model of foreland-basin sequences: Geology, v. 16, p. 501–504.
- Hendrix, M.S., Graham, S.A., Carroll, A.R., Sobel, E.R., McKnight, C.L., Schuelein, B.J., and Zuoxun Wang, 1992, Sedimentary record and climatic implications of recurrent deformation in the Tien Shan: Evidence from Mesozoic strata of the north Tarim, south Junggar, and Turpan basins, Northwest China: Geological Society of America Bulletin, v. 104, p. 53–79.
- Hendrix, M.S., Dumitru, T.A., and Graham, S.A., 1994, Late Oligocene–early Miocene unroofing in the Chinese Tien Shan: an early effect of the India-Asia collision: Geology, v. 22, p. 487–490.
- Hurfurd, A.J., and Green, P.F., 1983, The zeta calibration of fission-track dating: Chemical Geology (Isotope Geoscience Section), v. 1, p. 285–317.
- Ibragimov, A.Kh., and Turdukulov, A.T., 1965, Stratigrafii tretichnykh kontinental'nykh otlozheniy Chuyskoy vpadiny [Stratigraphy of the Tertiary continental deposits of the Chu Basin], in Koroliov, V.G., ed., Novyye dannyye po stratigrafii Tyan-Shanya [New data on the stratigraphy of the Tien Shan]: Frunze, Kyrgyzstan, Ilim Press, p.173–187.
- IVTAN, 1983, Depth to basement map: Block structure of the Frunze polygon: Bishkek, CCCP Academy of Sciences, scale 1:200 000, 1 sheet.
- Jordan, T.E., Flemings, P.B., and Beer, J.A., 1988, Dating thrust-fault activity by use of foreland-basin strata, in Kleinspehn, K.L., and Paola, C., eds., New perspectives in basin analysis: New York, Springer-Verlag, p. 307–330.
- Kirschvink, J.L., 1980, The least-squares line and plane and the analysis of palaeomagnetic data: Geophysical Journal of the Royal Astronomical Society, v. 62, p. 699–718.
- Krylov, A.Y., 1960, The absolute age of the rocks in the central Tyan-Shan and the application of argon method to metamorphic and sedimentary rocks, in determination of the absolute age of pre-Quaternary rocks: Moscow, An SSSR Press, Report of the International Geological Congress, p. 222–244.
- Lindsay, E.H., Opdyke, N.D., Johnson, N.M., 1980, Pliocene dispersal of the horse *Equus* and late Cenozoic mammalian dispersal events: Nature, v. 287, p. 135–138.
- McFadden, P.L., and McElhinny, M.W., 1990, Classification of the reversal test in paleomagnetism: Geophysical Journal International, v. 103, p. 725–729.
- Metivier, F., and Gaudemer, Y., 1997, Mass transfer between eastern Tien Shan and adjacent basins (Central Asia): constraints on regional tectonics and topography: Geophysical Journal International, v. 128, p. 1–17.
- Mikolaichuk, A.V., 2000, The structural position of trusts in the recent orogen of the Central Tien Shan: Russian Geology and Geophysics, v. 41, no. 7, p. 961–970.
- Molnar, P., and Deng, Q.D., 1984, Faulting associated with large earthquakes and the average rate of deformation in central and eastern Asia: Journal of Geophysical Research, v. 89, p. 6203–6228.
- Molnar, P., and England, P., 1990, Late Cenozoic uplift of mountain ranges and global climatic change: Chicken or egg?: Nature, v. 346, p. 29–34.
- Molnar, P., England, P., and Martinod, J., 1993, Mantle dynamics, uplift of the Tibetan Plateau, and the Indian monsoon: Reviews of Geophysics, v. 31, p. 357–396.
- Naeser, C.W., 1976, Fission-track dating: U.S. Geologic Survey Open-File Report 76–190, 65 p.
- Norin, E., 1941, Geologic reconnaissances in the Chinese Tien Shan: Reports from the scientific expedition to the northwest provinces of China under the leadership of Dr. Sven Hedin, (III), Geology 6: Stockholm, Ak-tiebolaget Thule, 229 p.
- O'Sullivan, P.B., and Parrish, R.R., 1995, The importance of apatite composition and single-grain ages when interpreting fission track data from plutonic rocks: A case study from the Coast Ranges, British Columbia: Earth and Planetary Science Letters, v. 132, p. 213–224.
- Sobel, E.R., and Dumitru, T.A., 1997, Thrusting and exhumation around the margins of the western Tarim basin during the Indian-Asia collision: Journal of Geophysical Research, v. 102B, p. 5043–5063.
- Tarasov, S.A., 1971, O stratigraficheskoy nomenklature paleogen-neogenovykh otlozheniy Severo-Vostochnoy Kirgizii: Mat-ly po noveysheму etapu geol. Razvitiya Tyan Shanya [Stratigraphic nomenclature of the Paleogene–Neogene deposits of northeastern Kirgizia; Information on the youngest stage of geologic development of the Tien Shan]: Frunze, Kyrgyzstan, Ilim Press, 112 p.
- Thompson, S., Weldon, R., III, Rubin, C., Abdрахmatov, K., and Anonymous, 1999, Late Quaternary river terraces provide kinematic tests for fault-related folding in the Kyrgyz Tien Shan, Central Asia: Geological Society of America Abstracts with Programs, v. 31, no. 7, p. 128.
- Trofimov, A.K., Udalov, H.P., Utkena, H.G., Fortuna, A.B., Chediya, O.K., and Yazovskii, B.M., 1976, Geologiya kaynozoya Chuyskoy vpadini i eyo gornogo obramleniya [Cenozoic geology of the Chu Basin and surrounding mountains]: Leningrad, Academia Nauk CCCP, p. 1–128.
- Windley, B.F., Allen, M.B., Zhang, C., Z-Y Zhao, and G-R Wang, 1990, Paleozoic accretion and Cenozoic reformation of the Chinese Tien Shan Range, Central Asia: Geology, v. 18, p. 128–131.
- Yin, A., Nie, S., Craig, P., Harrison, T.M., Ryerson, F.J., Qian Xianglin, Yang Geng, 1998, Late Cenozoic tectonic evolution of the southern Chinese Tien Shan: Tectonics, v. 17, p. 1–27.

MANUSCRIPT RECEIVED BY THE SOCIETY OCTOBER 20, 1999
 REVISED MANUSCRIPT RECEIVED MARCH 1, 2000
 MANUSCRIPT ACCEPTED MAY 16, 2001

Printed in the USA